Multidimensional Random Walk for Calculating the Fusion/Fission Probabilities of Superheavy Elements

Aleksander Augustyn

Michał Kowal, Tomasz Cap, Krystyna Siwek-Wilczyńska

NATIONAL CENTRE FOR NUCLEAR RESEARCH
ŚWIERK

10.10.2024
Graduate Physics Seminar

PHYSICAL REVIEW C **109**, L061603 (2024)

Letter

Dipole-driven multidimensional fusion: An insightful approach to the formation of superheavy nuclei

T. Cap[1,*] A. Augustyn[1] M. Kowal[1] and K. Siwek-Wilczyńska[2]

[1] *National Centre for Nuclear Research, Pasteura 7, 02-093 Warsaw, Poland*

[2] *Faculty of Physics, Warsaw University, Pasteura 5, 02-093 Warsaw, Poland*

(Received 6 February 2024; accepted 3 June 2024; published 28 June 2024)

We present an approach to describe the fusion of two heavy ions in which the colliding system has access to a wide spectrum of shapes through the utilization of an auxiliary reference frame and the employment of a multipole expansion of the nuclear radius with the dipole term treated as an actual and leading shape variable. Access to fusion shapes that would otherwise be unattainable is possible by initially placing the origin of the auxiliary reference frame in the neck region between the colliding nuclei. The fusion process is modeled as an unconstrained biased random walk in a four-dimensional deformation space with step probabilities correlated to the density of available states. Deformation energy is calculated using the macroscopic-microscopic method, incorporating rotational energy. The presented approach successfully describes fusion probabilities for reactions involving ^{48}Ca, ^{50}Ti, and ^{54}Cr projectiles with a ^{208}Pb target.

DOI: 10.1103/PhysRevC.109.L061603

Superheavy elements

- Only man-made
- Z>103 (transactinides)
- Produced in nuclear reactions:
  - Cold fusion
  - Hot fusion

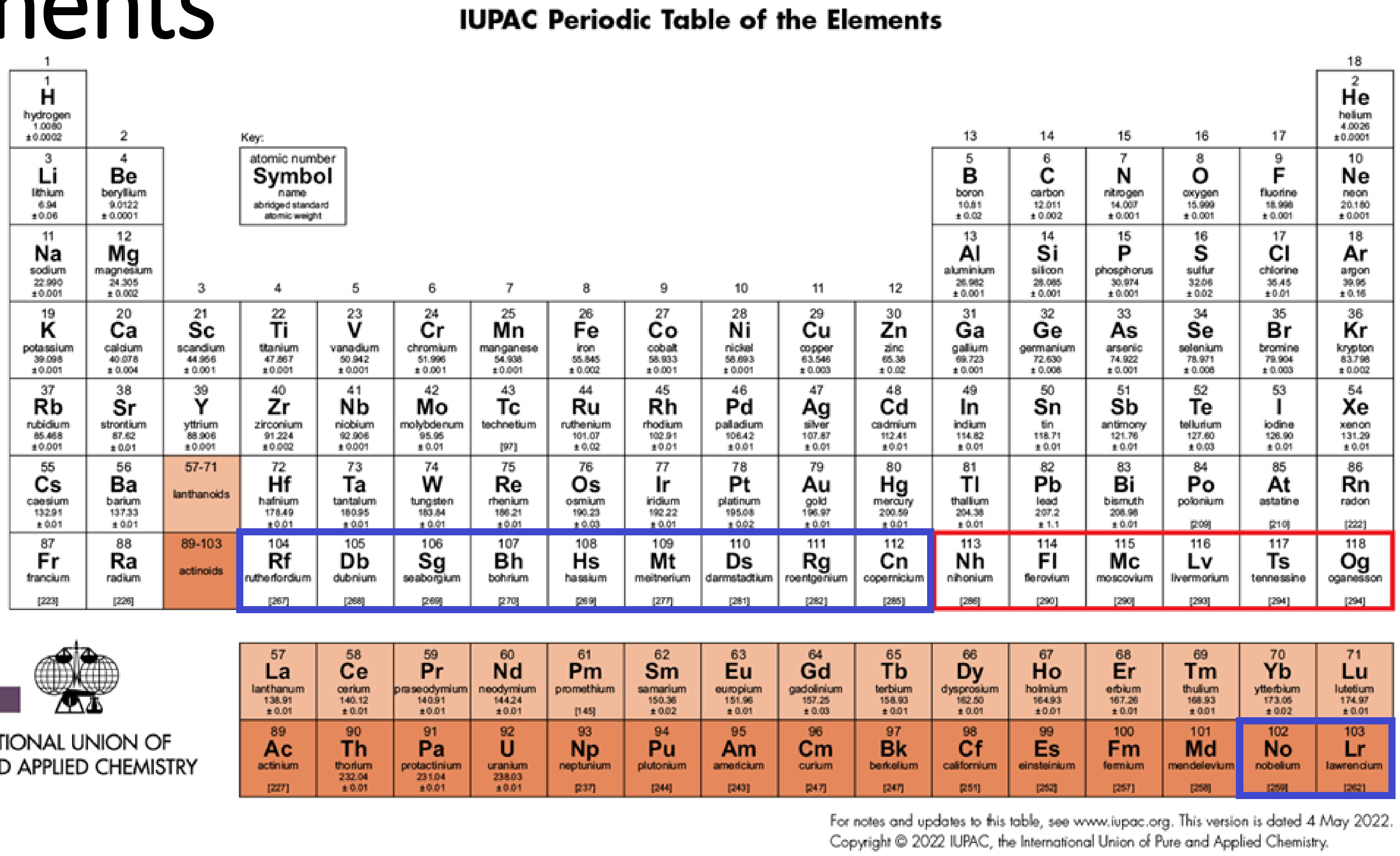

INTERNATIONAL UNION OF PURE AND APPLIED CHEMISTRY

Superheavy elements

Oganessian, Yu. (2006). Synthesis and decay properties of superheavy elements. Pure and Applied Chemistry - PURE APPL CHEM. 78. 889-904. 10.1351/pac200678050889.

- Only man-made
- Z>103 (transactinides)
- Produced in nuclear reactions:
  - Cold fusion
  - Hot fusion

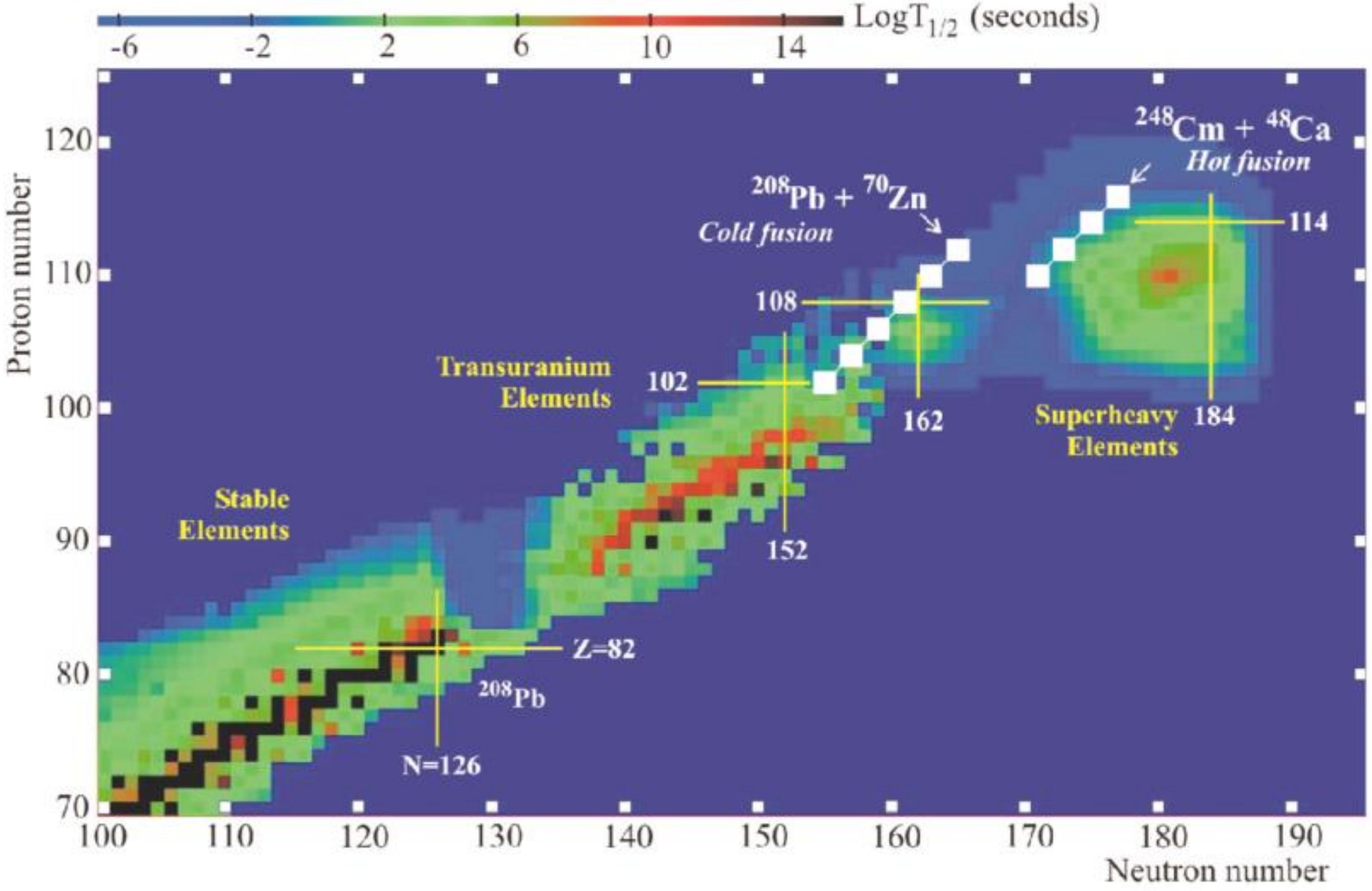

Cold and hot fusion

- $E^* \approx$ 10-20 MeV
- Compound system is only weakly heated and is cooled down via emission of just one or two neutrons
- Magic nuclei as targets (spherical shapes)

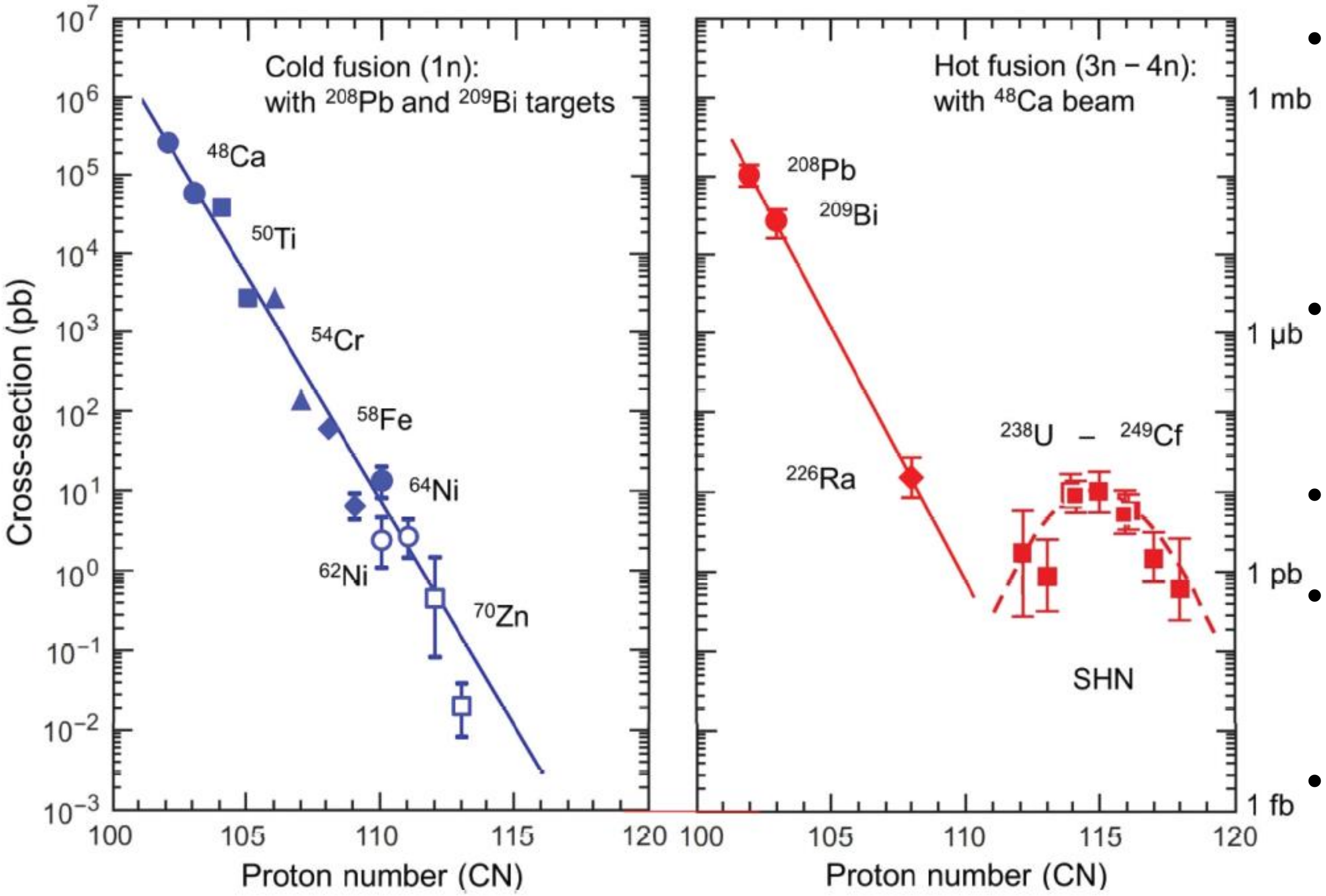

Sigurd Hofmann, Sergey N. Dmitriev, Claes Fahlander, Jacklyn M. Gates, James B. Roberto and Hideyuki Sakai
Report of the 2017 Joint Working Group of IUPAC and IUPAP, Pure Appl. Chem. 2020; 92(9): 1387–1446

- $E^* \approx$ 30-40 MeV
- Compound nucleus is quite excited (most often emits 3 neutrons)
- Well-deformed radioactive actinides (Act.) targets
- Doubly magic projectile ^{48}Ca
- Heavier actinides with Z>98 too short-lived to be used as targets
- Attempts of going beyond the reactions Act. + ^{48}Ca by using heavier projectiles (like ^{50}Ti, ^{54}Cr, ^{58}Fe, ^{64}Ni) gave no results so far.

Motivation

- Find the mechanism responsible for the 7 orders of magnitude decrease of cross section
- We wanted to use the Warsaw micro-macro model with the inclusion of rotational energy and a multidimensional, biased, unconstrained random walk method on potential energy surfaces (PES) to calculate the probability of fusion, while describing the fusion /fission processes
- The model was first tested on cold fusion reactions with near spherical projectiles: $^{48}Ca+^{208}Pb$, $^{50}Ti+^{208}Pb$ and $^{54}Cr+^{208}Pb$ in a wide range of excitation energies

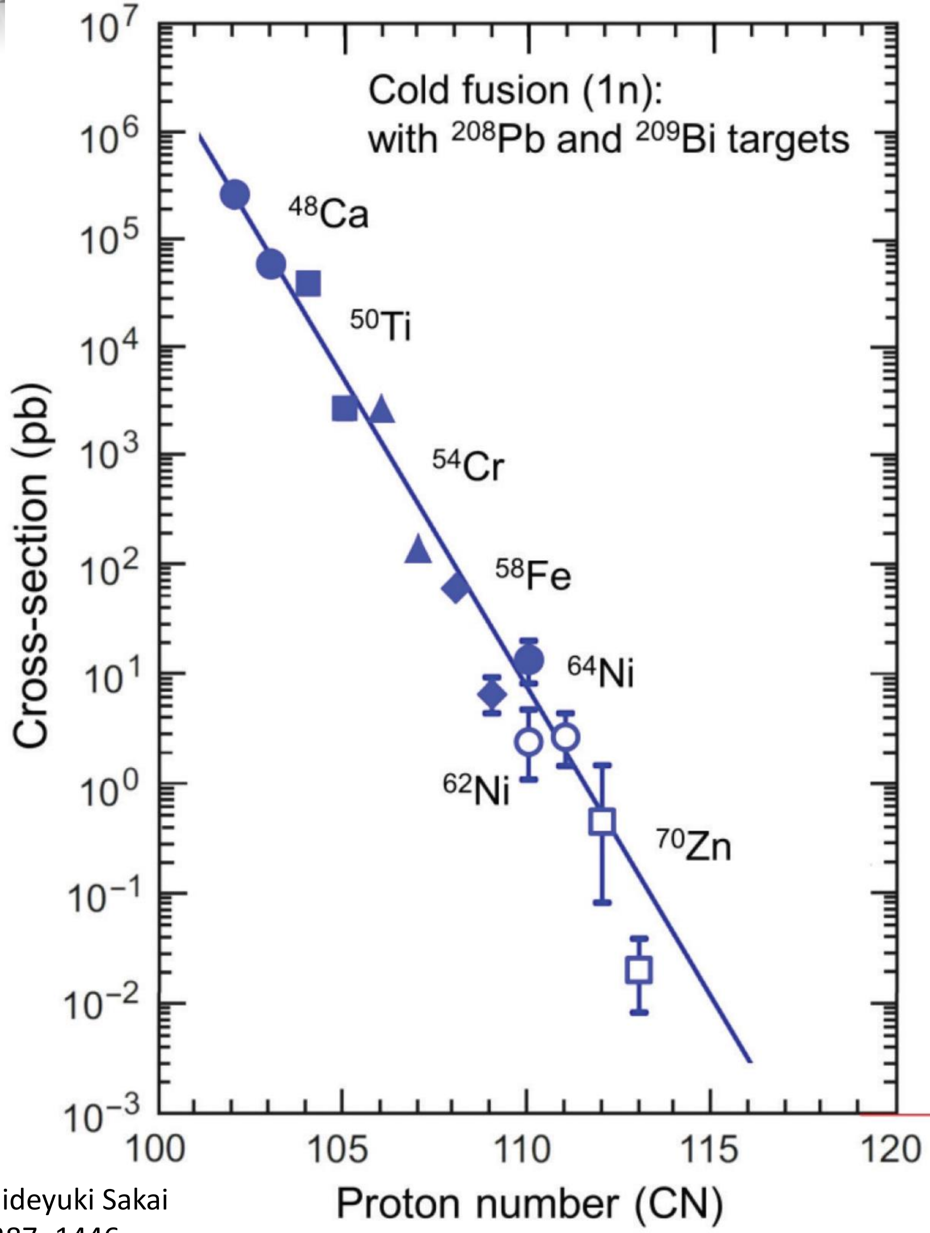

Sigurd Hofmann, Sergey N. Dmitriev, Claes Fahlander, Jacklyn M. Gates, James B. Roberto and Hideyuki Sakai
Report of the 2017 Joint Working Group of IUPAC and IUPAP, Pure Appl. Chem. 2020; 92(9): 1387–1446

Synthesis model

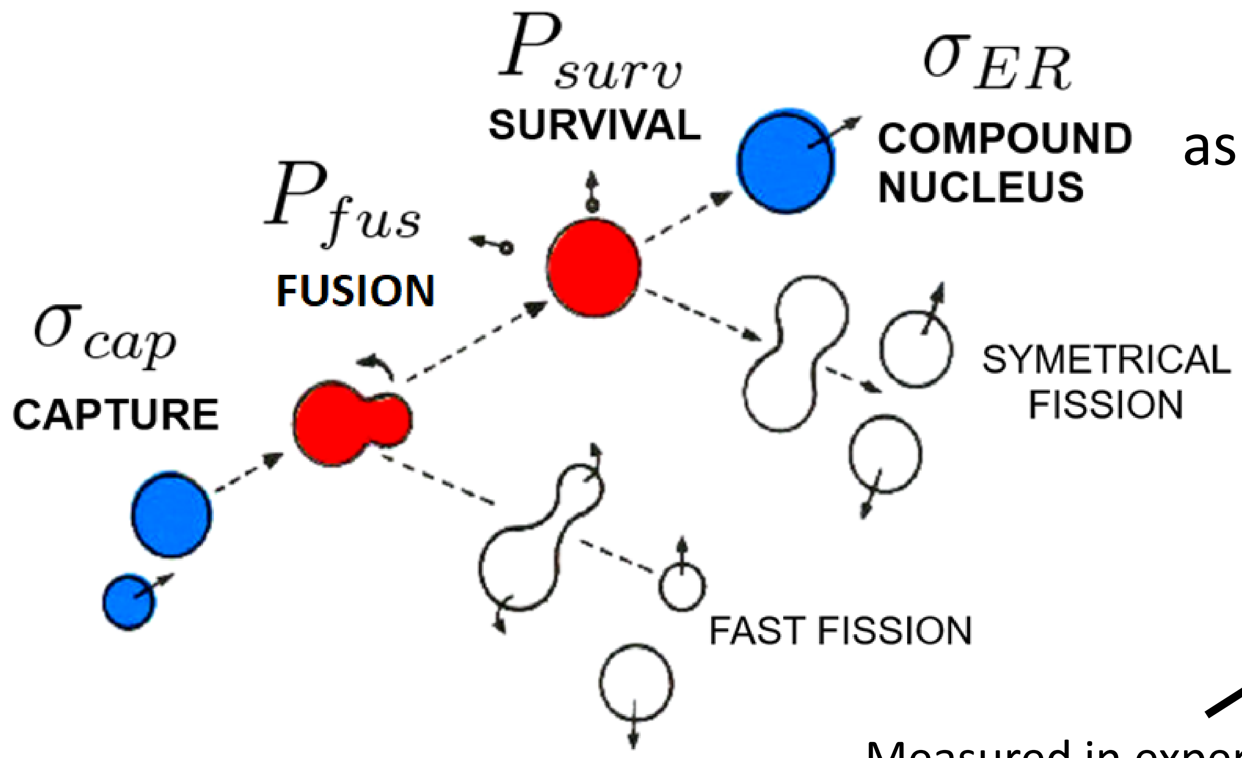

Synthesis of SHN can be described as a **3** step process, due to the different timescales of the particular reaction stages:

$$\sigma_{ER} = \sigma_{cap} \; P_{fus} \; P_{surv}$$

Measured in experiments, can be calculated using various models

Not measured directly, difficult to calculate

Well established theory and formulas
Monte Carlo Statistical model
$P_{surv} << 1$

Diffused barrier formula (Entrance channel barrier is given by a Gaussian distribution)

Smoluchowski Diffusion Equation, Random Walk

masses, fission barriers, deformations from Warsaw Micro-Macro model

W. J. Świątecki, K. Siwek-Wilczyńska, J. Wilczyński, **PRC 2005**
T. Cap et al., **PRC 2011**
K. Siwek-Wilczyńska et al. **PRC 2012**
T. Cap et al., **PRC 2013**
K. Siwek-Wilczyńska et al. **PRC 2019**

Capture cross section σ_{cap}

- The entrance channel barrier is described by a distribution that can be approximated by a Gaussian function
- The formula for the capture cross section is derived by folding the Gaussian barrier distribution with the classical expression for the fusion cross section

$$\sigma_{cap} = \pi R^2 \frac{\omega}{E_{c.m.}\sqrt{2\pi}} \left[X\sqrt{\pi}(1+\mathrm{erf}(X)) + \exp(-X^2) \right] =$$
$$= \pi \lambdabar^2 (2l_{max}+1)^2, \quad \text{where } X = \frac{E_{c.m.} - B_0}{\omega\sqrt{2}}$$

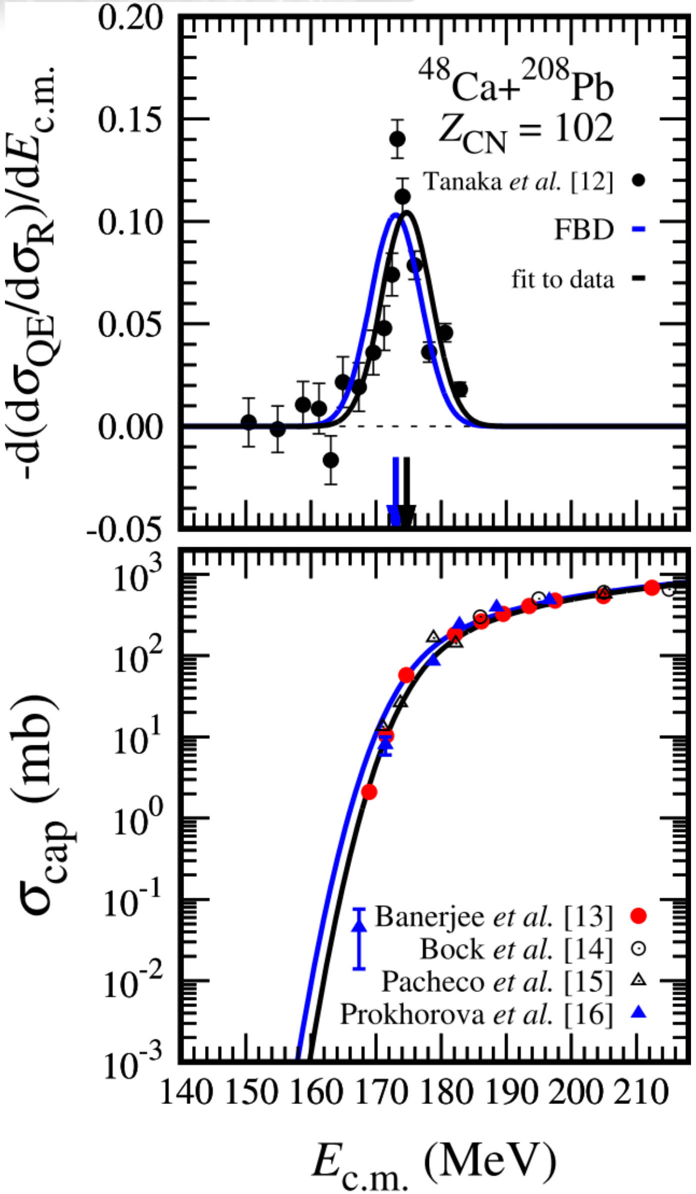

Cap, T., Kowal, M. & Siwek-Wilczyńska, K. The Fusion-by-Diffusion model as a tool to calculate cross sections for the production of superheavy nuclei. *Eur. Phys. J. A* **58**, 231 (2022).

NARODOWE CENTRUM BADAŃ JĄDROWYCH ŚWIERK

P_{fus} in experiment

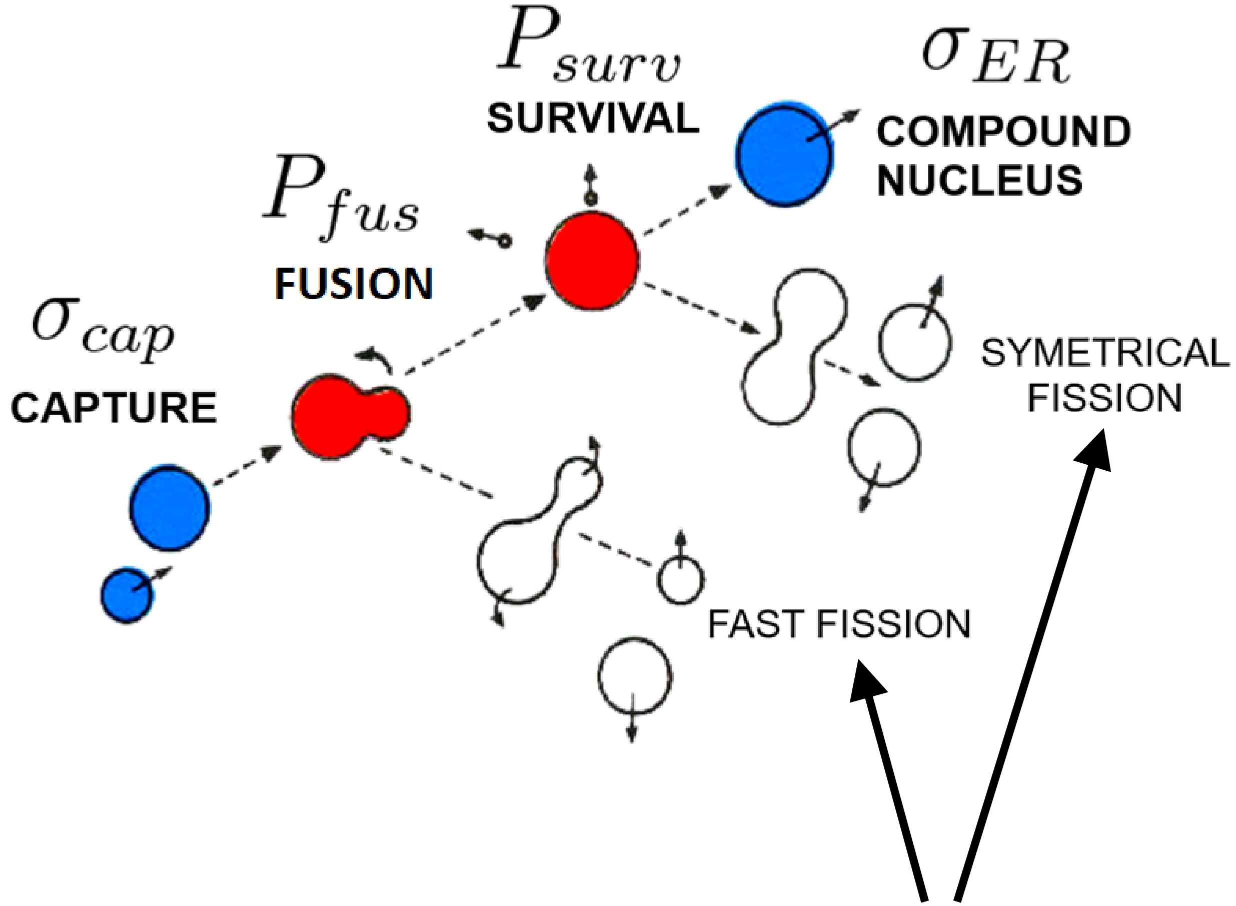

measured in the experiment

Mechanisms Suppressing Superheavy Element Yields in Cold Fusion Reactions
Banerjee *et al.*, PRL 122, 232503 (2019)

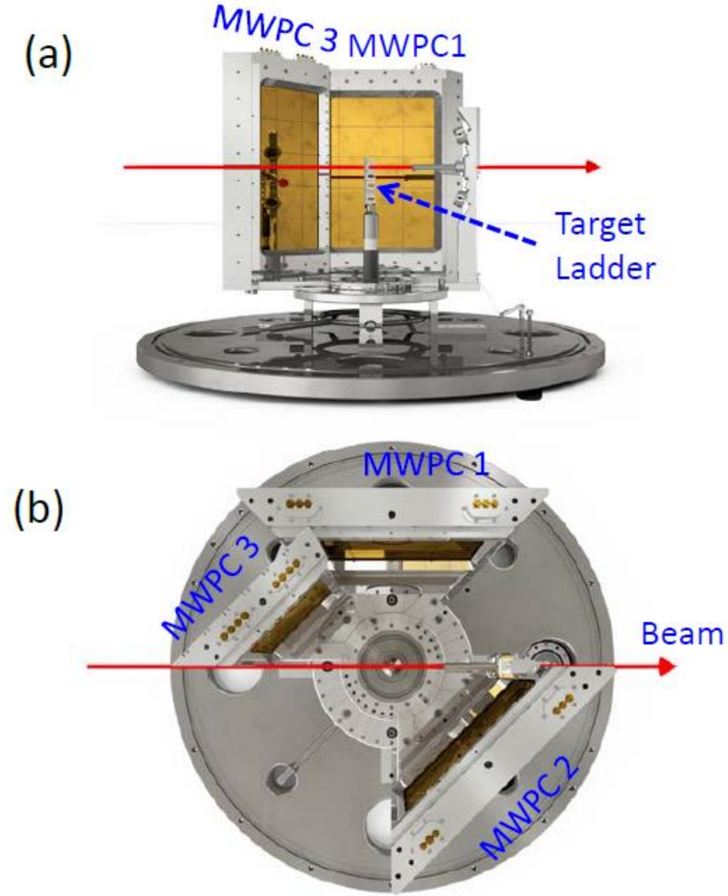

P_{fus} in experiment

Mechanisms Suppressing Superheavy Element Yields in Cold Fusion Reactions
Banerjee *et al.*, PRL 122, 232503 (2019)

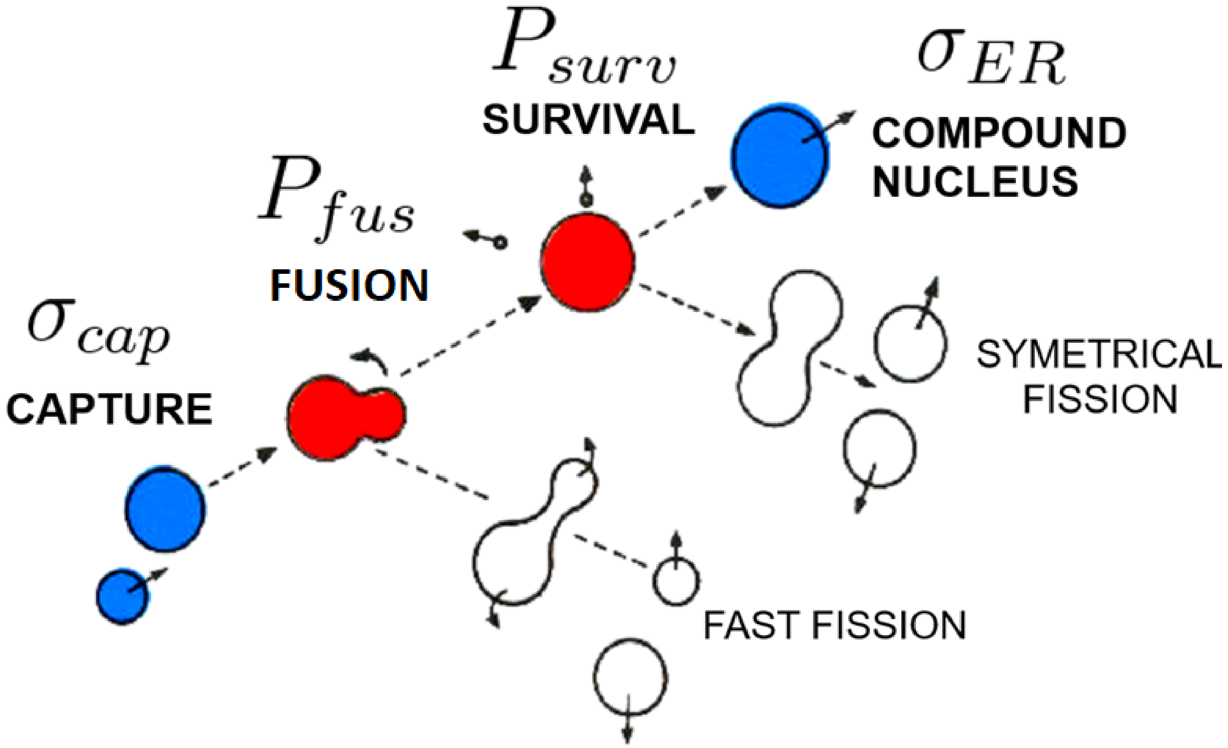

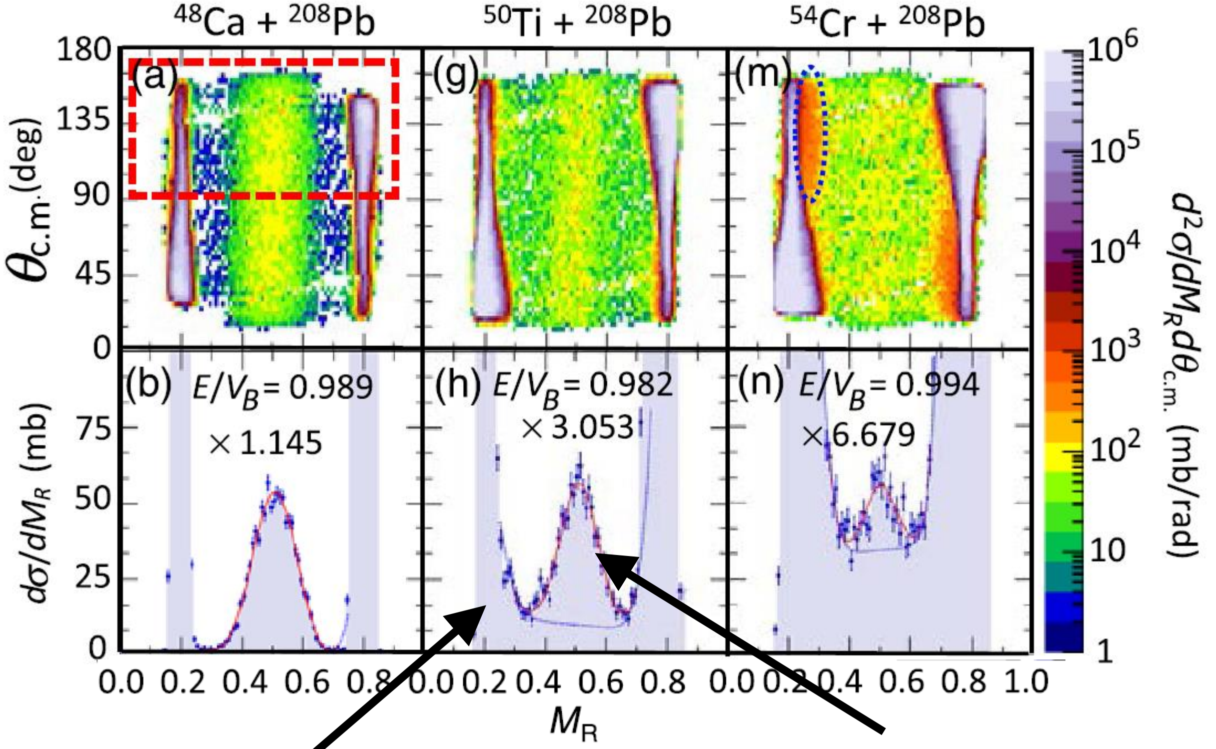

Fast Fission cross section

Mass ratio, Symmetric split: $M_R = 0.5$

Fusion-Fission cross section (symmetrical fission)

P_{fus} can be experimentally estimated:

$$P_{sym} = \frac{\textbf{Fusion–Fission}\text{ cross section}}{\textbf{Capture}\text{ cross section}}$$

Banerjee et al., PRL 122, 232503 (2019)

Reactions:

$^{48}Ca + ^{208}Pb \rightarrow ^{256}No^*$

$^{50}Ti + ^{208}Pb \rightarrow ^{258}Rf^*$

$^{54}Cr + ^{208}Pb \rightarrow ^{262}Sg^*$

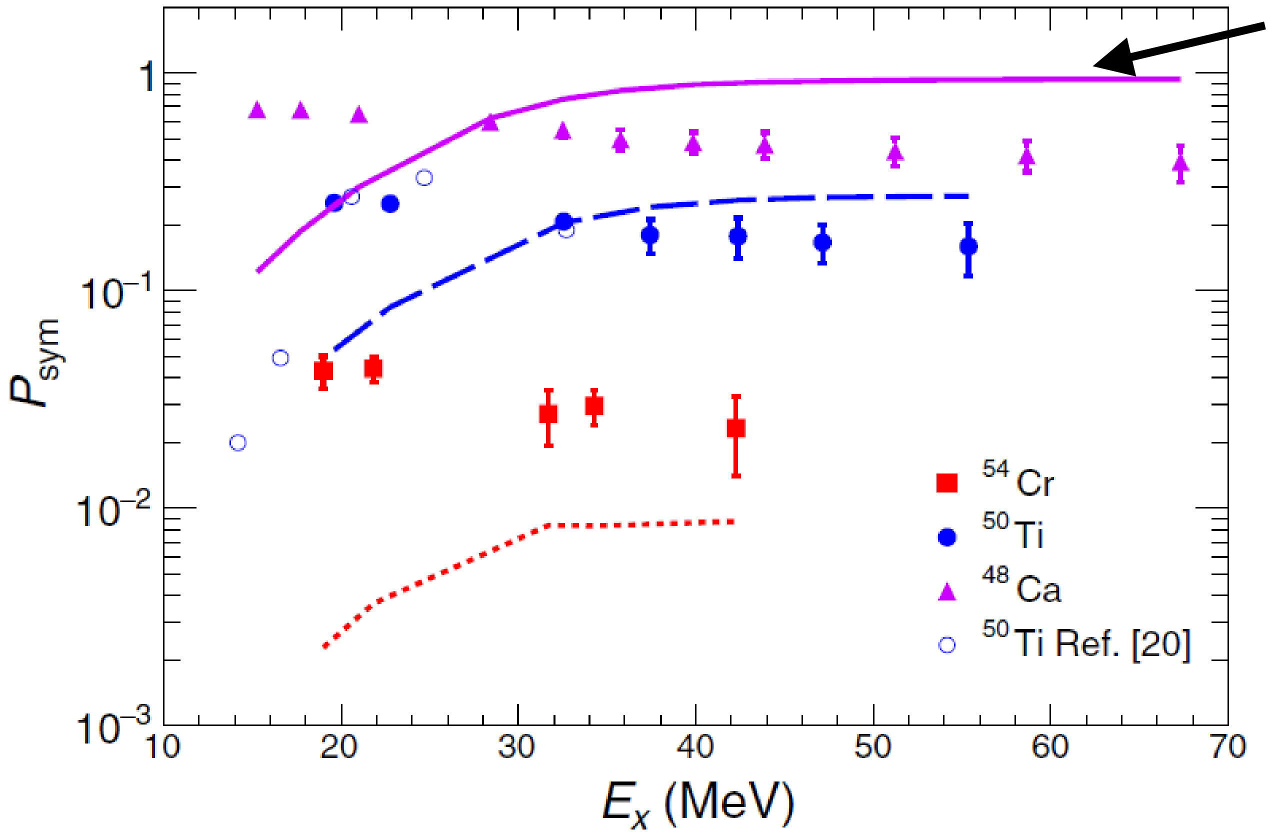

Upper limit for fusion probability

Excitation energy

Diffusion model calculations by V. Zagrebaev and W. Greiner PRC 78, 034610 (2008).

The experimental trends are different than the model predictions for all 3 reactions.

The conclusion was that diffusion is not the main mechanism responsible for the synthesis of SHN.

NARODOWE CENTRUM BADAŃ JĄDROWYCH ŚWIERK

P_{fus} in Fusion by Diffusion

1D motion approximation
The system must overcome an internal barrier ***H*** to fuse.

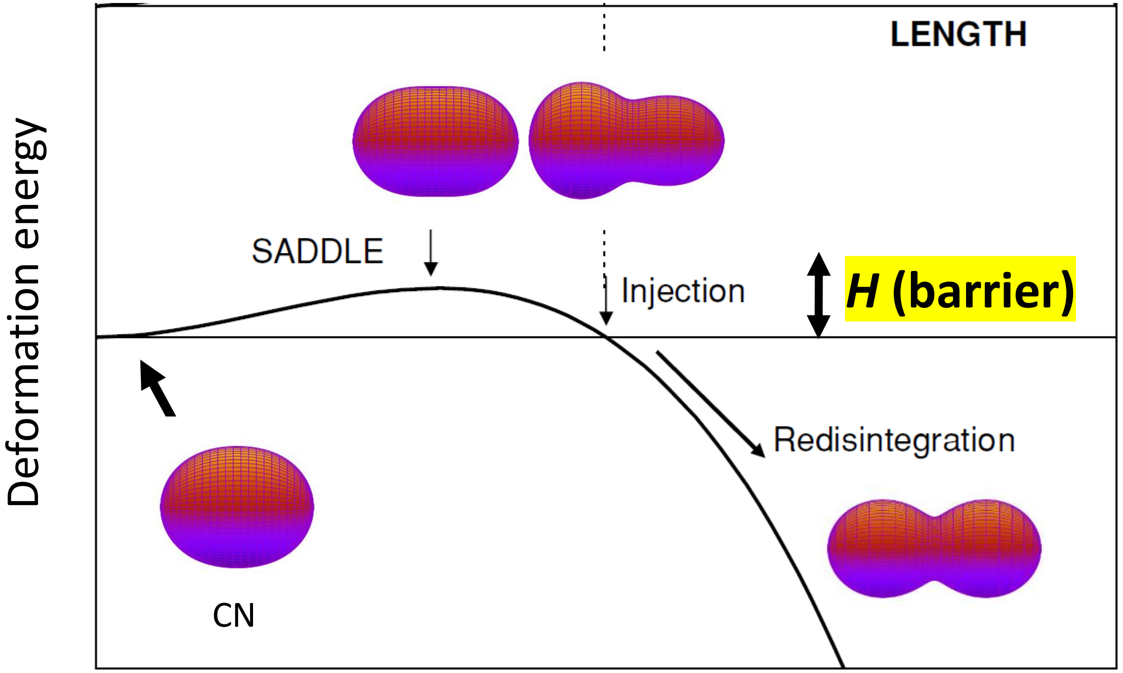

L is the effective elongation (along the fusion path)

P_{fus} is calculated by solving
1D Smoluchowski Diffusion Equation

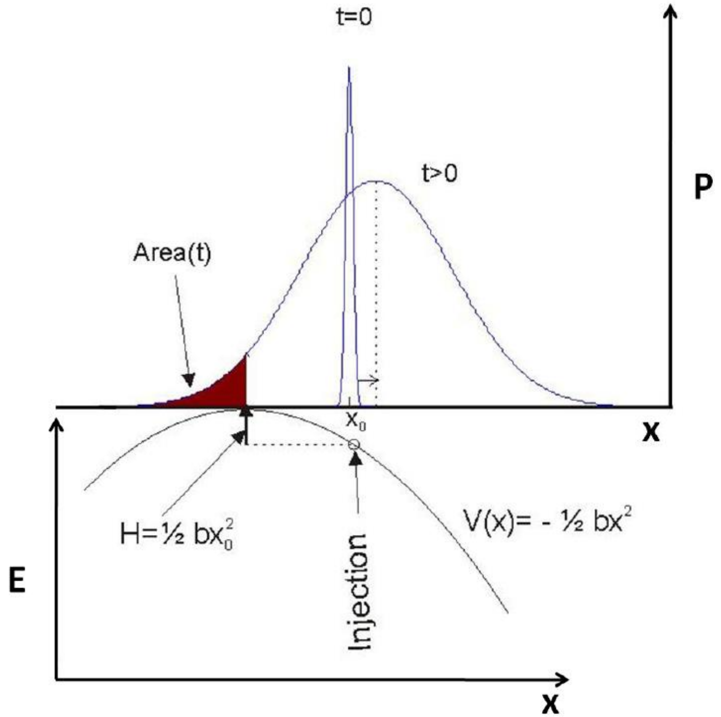

$$P_{fus}(l) = \frac{1}{2}\left(1 - \mathrm{erf}\left(\sqrt{\frac{H(l)}{T}}\right)\right) \text{ when } L_{inj} \geq L_{saddle}$$

H(l) – the function of angular momentum and bombarding energy
T – the temperature depends on available energy

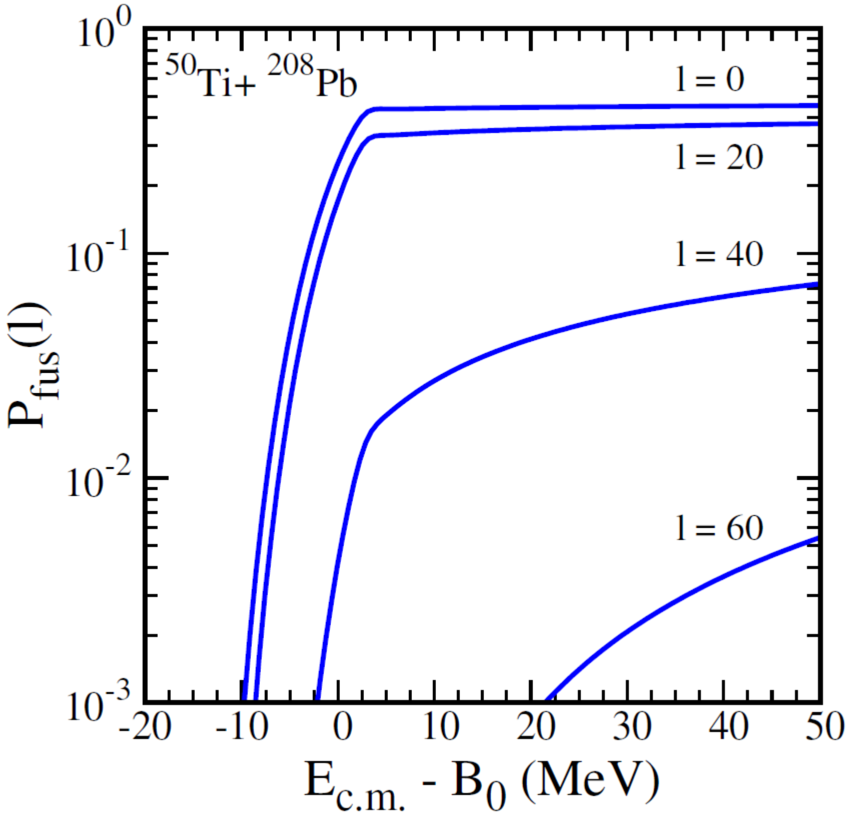

Energy relative to the entrance channel barrier B_0

$l = 0$
Central collision

Peripheral collisions

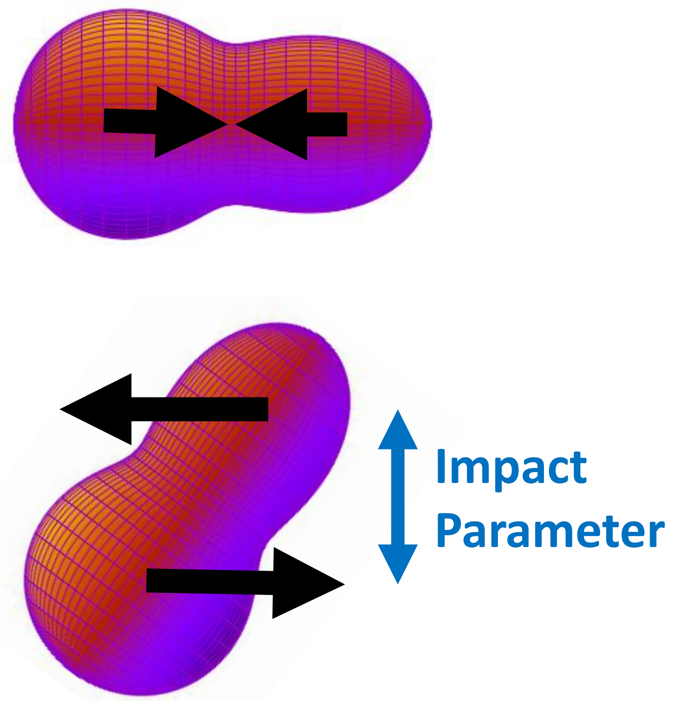

$B_0 = 191.3$ MeV
$E^*(E_{c.m.} = B0) = 21.7$ MeV

Higer partial waves l
=
Higher rotational energy
=
Higher barrier $H(l)$
=
Lower $Pfus(l)$

Fusion probability from FbD model

- Highly effective phenomenological approach
- Only takes into account the macroscopic energy
- Limited to 1 shape dimension (elongation)

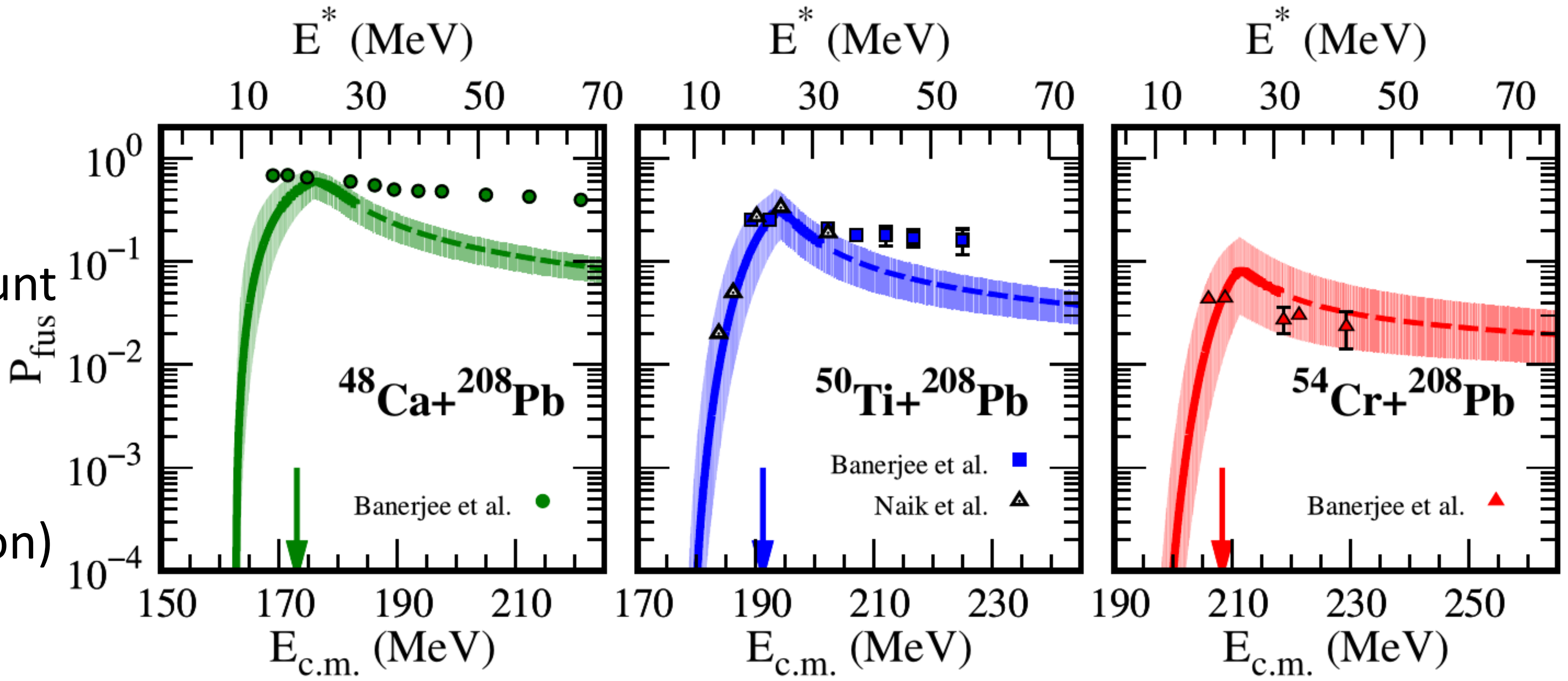

T. Cap, M. Kowal, and K. Siwek-Wilczyńska, Phys. Rev. C **105**, L051601 (2022)

Features of the new model

- Using multidimensional deformation space, including the dipole
- Adopting an auxiliary reference frame giving access to otherwise unattainable shapes, specifically the starting configuration
- Adding the shell effect and rotational energy to the whole deformation space
- Replacing the Smoluchowski diffusion equation with a biased, unconstrained random walk

Goals of the new model

- Comparison with fragment mass distributions (fission, fusion-fission, quasi-fission) and TKE (total kinetic energy) distributions from experiments
- Study of the competition between fusion-fission and quasi-fission
- Study of the shape evolution during fusion and fission
- Modeling the effect of angular momentum on fusion, fission and quasi-fission
- Prediction of fusion probabilities for new SHE synthesis reactions

Binding/Potential energy in SHE

- Macroscopic (liquid drop) and microscopic (shell effects) energy
- liquid drop model is a phenomenological approach that likens the nucleus to a drop of incompressible fluid
- shell model posits that, as quantum objects, nucleons exist in discrete energy levels or shells, similar to electrons in atoms
- Shell effects responsible for superdeformed minimum in actinides
- SHE exist thanks to the shell effects creating the ground state (often deformed)
- <u>The model needs to account for both energies</u>

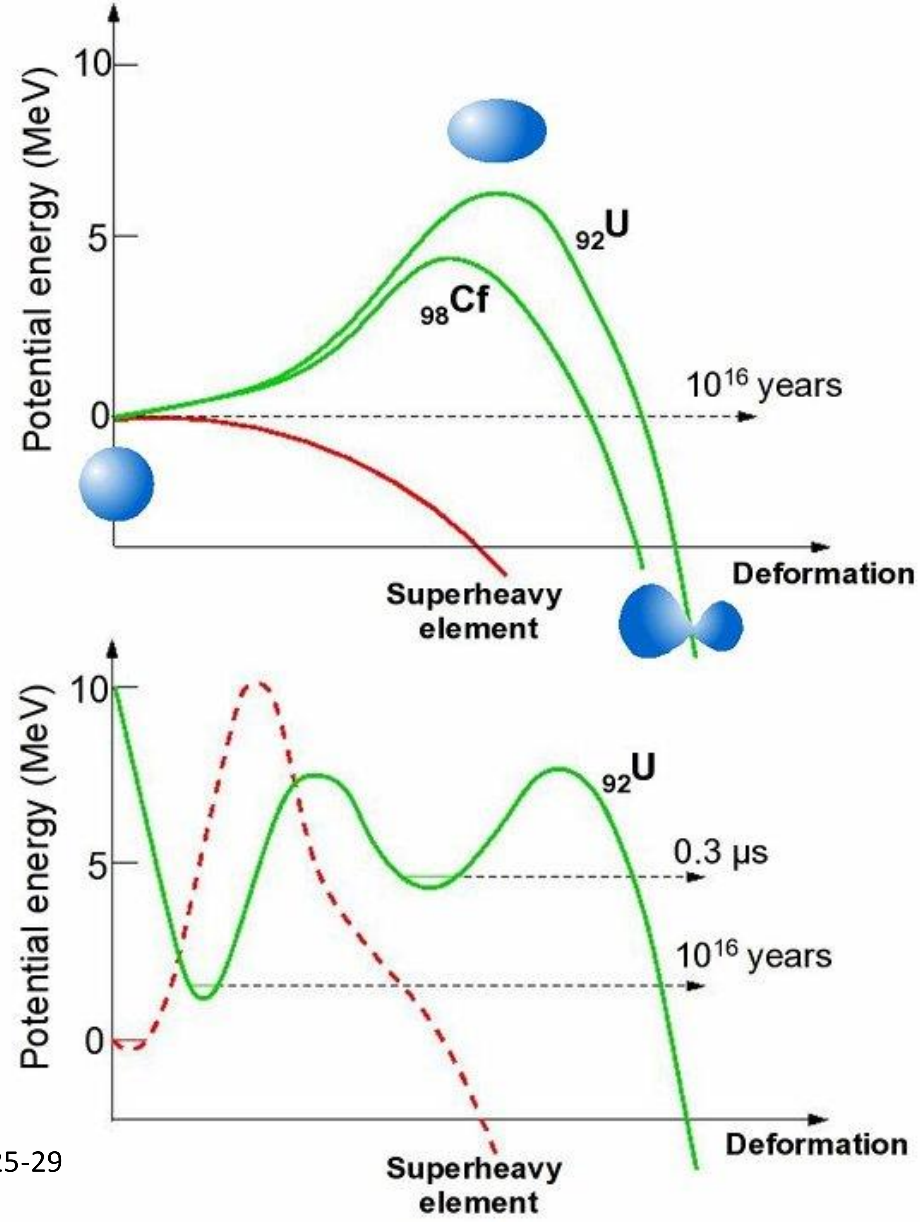

Oganessian, Yu. (2004). Superheavy elements. Physics World, 17(7), 25-29

Atomic Data and Nuclear Data Tables 138 (2021) 101393

Contents lists available at ScienceDirect

Atomic Data and Nuclear Data Tables

journal homepage: www.elsevier.com/locate/adt

Properties of heaviest nuclei with $98 \leq Z \leq 126$ and $134 \leq N \leq 192$

P. Jachimowicz [a], M. Kowal [b,*], J. Skalski [b]

[a] Institute of Physics, University of Zielona Góra, Szafrana 4a, 65-516 Zielona Góra, Poland
[b] National Centre for Nuclear Research, Pasteura 7, 02-093 Warsaw, Poland

Ground-state and saddle-point shapes and masses for 1305 heavy and superheavy nuclei
including odd-A and odd–odd systems. Static fission barrier heights, one- and two-nucleon separation energies, and Qα values.

Microscopic–macroscopic method with the deformed Woods–Saxon single-particle potential and the Yukawa-plus-exponential macroscopic energy taken as the smooth part.

Ground-state shapes and energies are found by the minimization over **seven axially-symmetric deformations**.
A search for saddle-points was performed by using the "imaginary water flow" method in three consecutive stages, using five- (for nonaxial shapes) and seven-dimensional (for reflection-asymmetric shapes) deformation spaces.

Good agreement with the experimental data for actinides.

Warsaw macro-micro model

liquid drop with a Yukawa-plus-exponential model

Strutinsky shell correction + Woods-Saxon potential + BCS

$$E_{tot}(Z,N,\beta) = E_{mac}(Z,N,\beta) + E_{mic}(Z,N,\beta)$$

$$E_{rot} = l(l+1)\frac{(\hbar c)^2}{2I(\beta)}$$

Rigid body approximation

- <u>Allows to obtain the binding energy for a given nuclear shape β</u>
- Macroscopic energy normalized with respect to the sphere:

$$E_{mac} = E_{mac}(deformation) - E_{mac}(sphere)$$

Shape parametrization

- An expansion of the nuclear radius R(θ, ϕ) onto spherical harmonics $Y_{\lambda\mu}$(θ, ϕ) is used:

$$R(\vartheta) = cR_0\left\{1 + \sum_{\lambda=1}^{\infty} \beta_{\lambda 0} Y_{\lambda 0}(\vartheta)\right\}$$

- For now, shapes in calculations are limited to axially symmetrical (μ = 0)

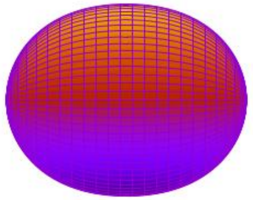

Compound nucleus

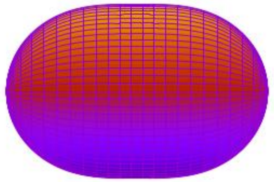

Fission saddle point

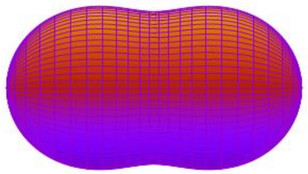

2nd minimum

Deformation parameters

- β_{10} – dipole, used as an actual shape parameter
- β_{20} – quadrupole/elongation
- β_{30} – octupole/asymmetry
- β_{40} –hexadecapole/neck parameter

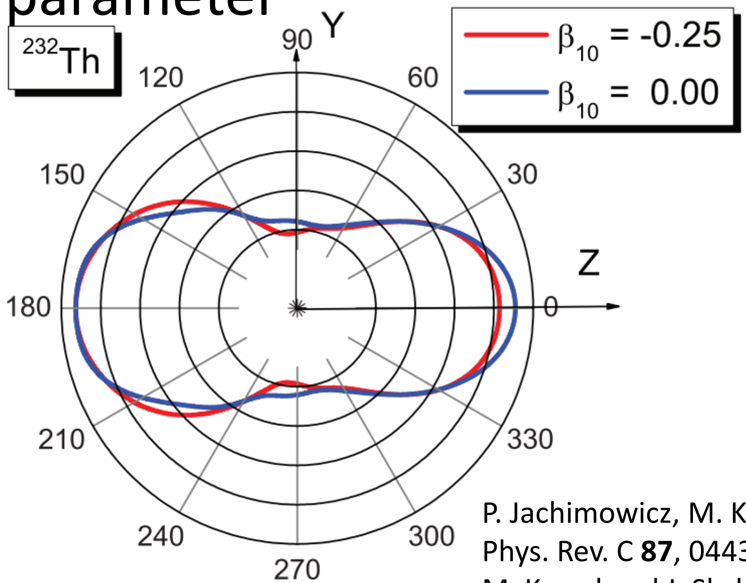

Third minimum, with and without β_{10}

P. Jachimowicz, M. Kowal, and J. Skalski, Phys. Rev. C **87**, 044308 (**2013**)
M. Kowal and J. Skalski, Phys. Rev. C **85**, 061302(R) (**2012**)

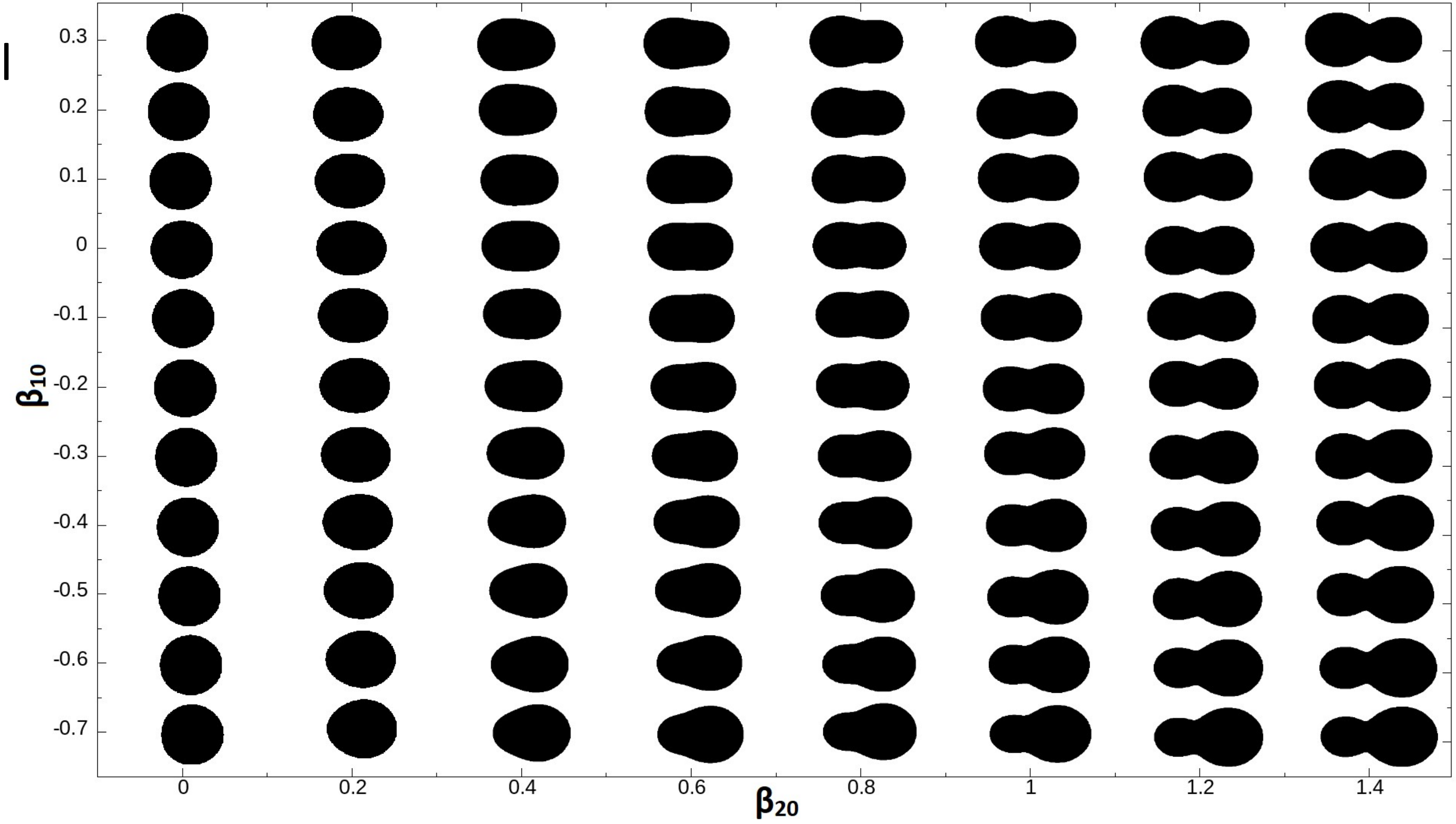

Dependance of shapes on β_{10} and β_{20} , other β=0

Deformation parameters

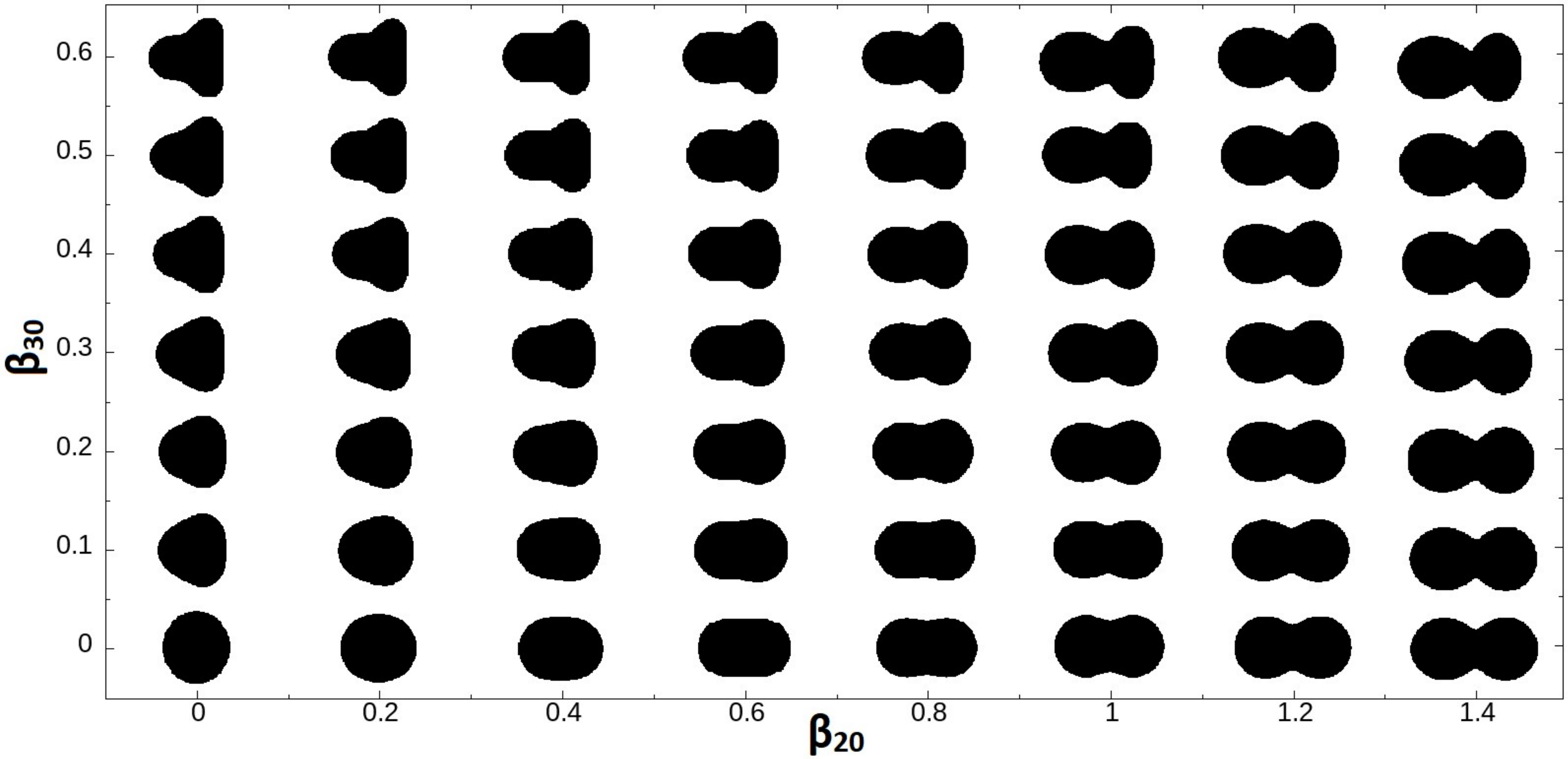

Deformation parameters

- β_{40} is crucial in the beginning of the fusion process and during scission

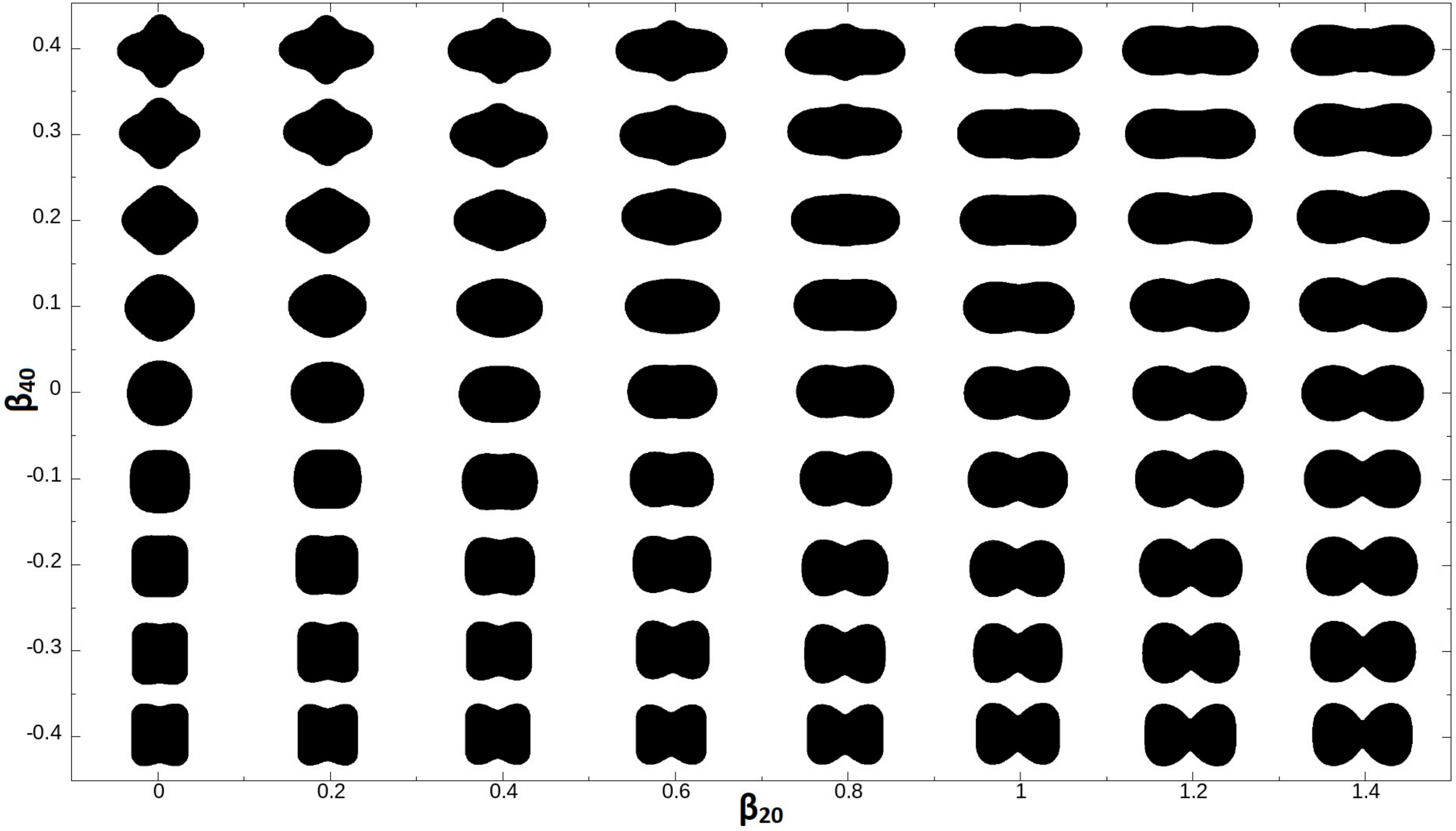

Starting point parametrization

- After overcoming the entrance channel barrier, the projectile and the target are assumed to be spherical and in a touching configuration
- The spherical harmonic parametrization is fitted, <u>with the origin situated in the neck</u>, giving the β parameters for the starting point configuration
- For now calculations are limited to 4 dimensions (β_{10} - β_{40})
- Currently working on expanding to 6 dimensions (β_{10} – β_{60})

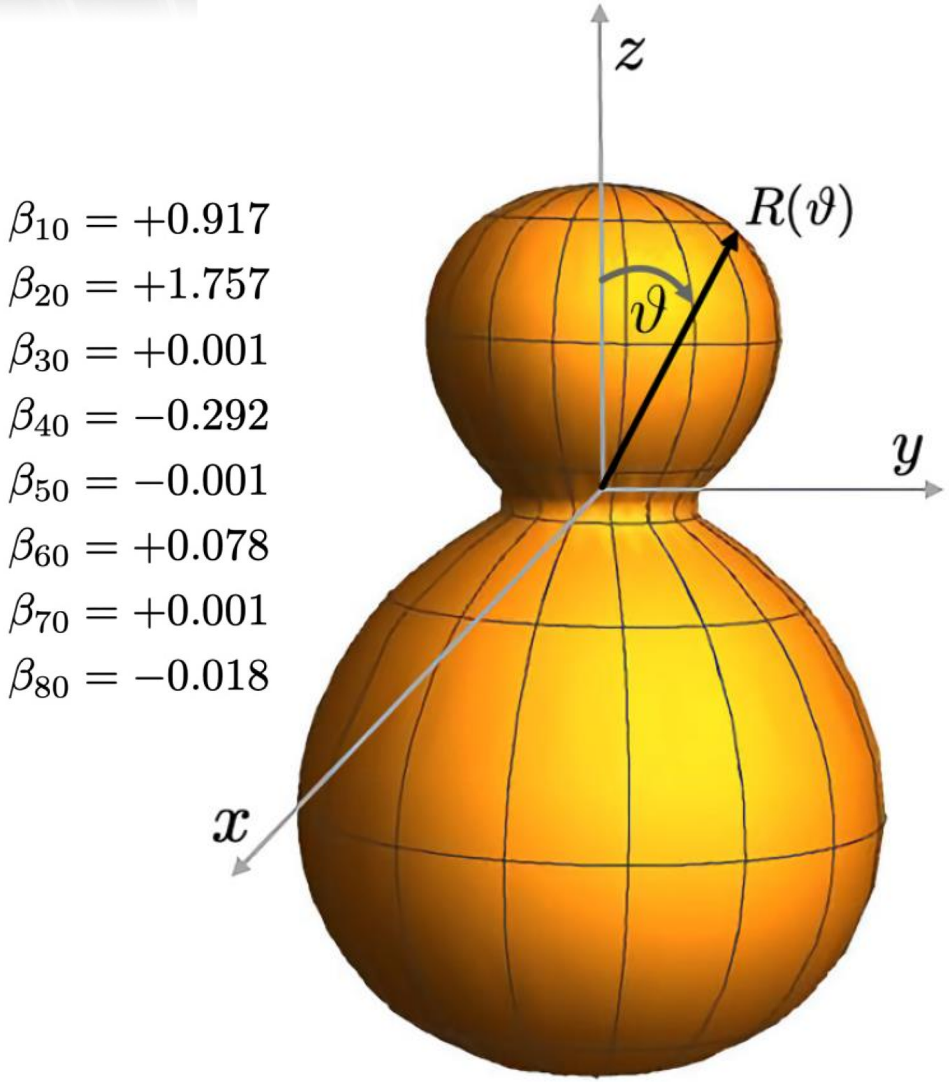

The initial fusion configuration for the $^{50}Ti+^{208}Pb$ system.
T. Cap, A. Augustyn, M. Kowal and K. Siwek-Wilczyńska, Phys. Rev. C **109**, L061603 (**2024**)

NARODOWE CENTRUM BADAŃ JĄDROWYCH ŚWIERK

What do we have?

- We have a parametrization to describe many nuclear shapes
- We can calculate the macroscopic, microscopic and rotational energy for those shapes, giving us PESs for different values of angular momentum
- We can determine the starting configuration of the fusion process

Now all we need is a way to move on the PESs from one shape to another

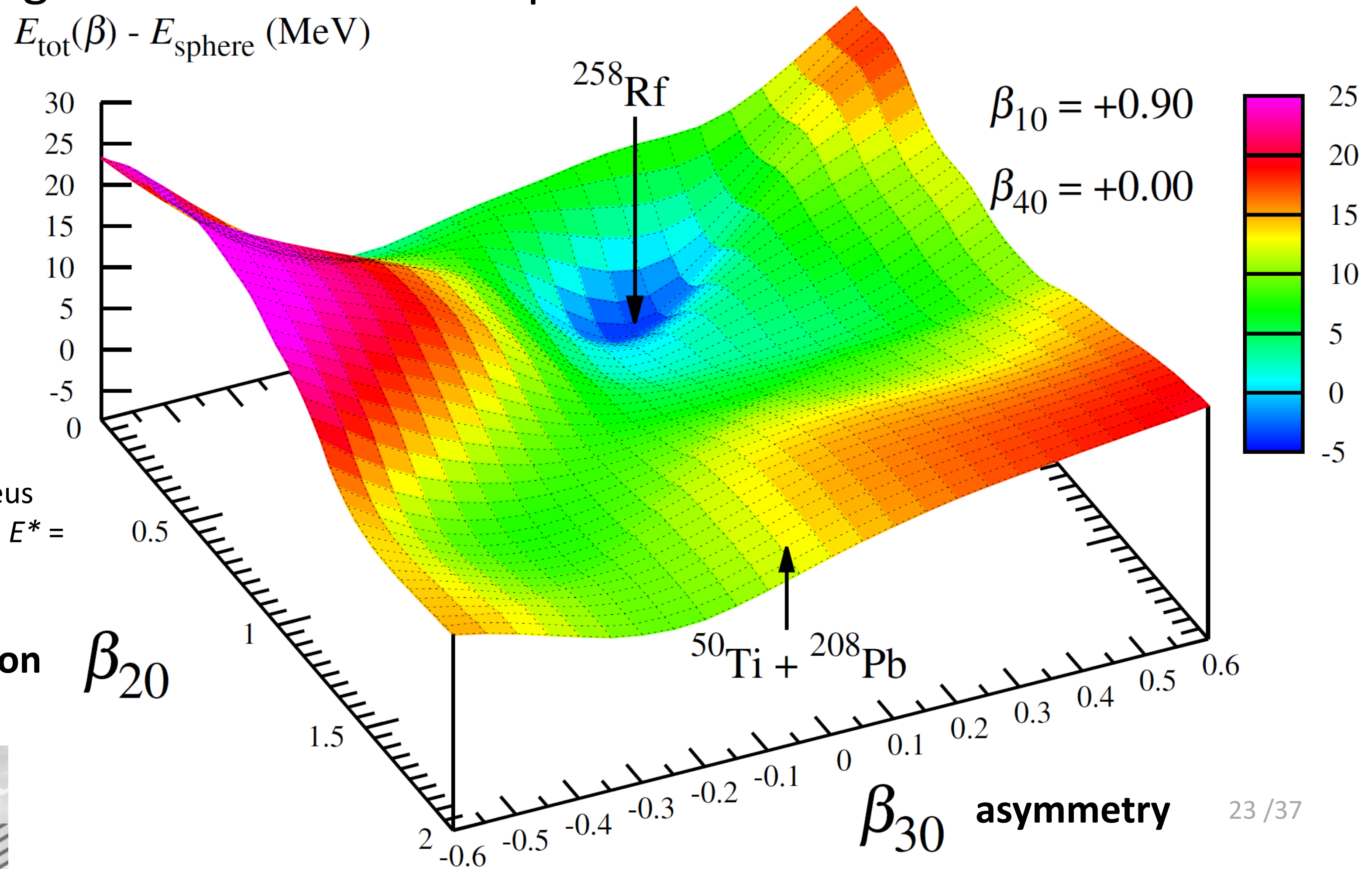

A fragment of the potential energy map for the ^{258}Rf nucleus calculated within the macroscopic-microscopic model. *E** = 20 MeV, *l*=0*ħ*.

NARODOWE CENTRUM BADAŃ JĄDROWYCH ŚWIERK

Biased, unconstrained random walk method

- The probability of transitioning from one shape to another is determined by the number of available energy levels for a given shape β -> <u>biased</u>

$$N_i(\beta_i,\ell) \propto \exp\left(2\sqrt{a\left(E^*_{\max}(\beta_i) - E_{\mathrm{rot}}(\beta_i,\ell)\right)}\right)$$

$a = \frac{A}{8.5}$ – constant nuclear level density parameter

- Only one β parameter changes at a time, by a step of 0.05, giving 8 possible directions of movement

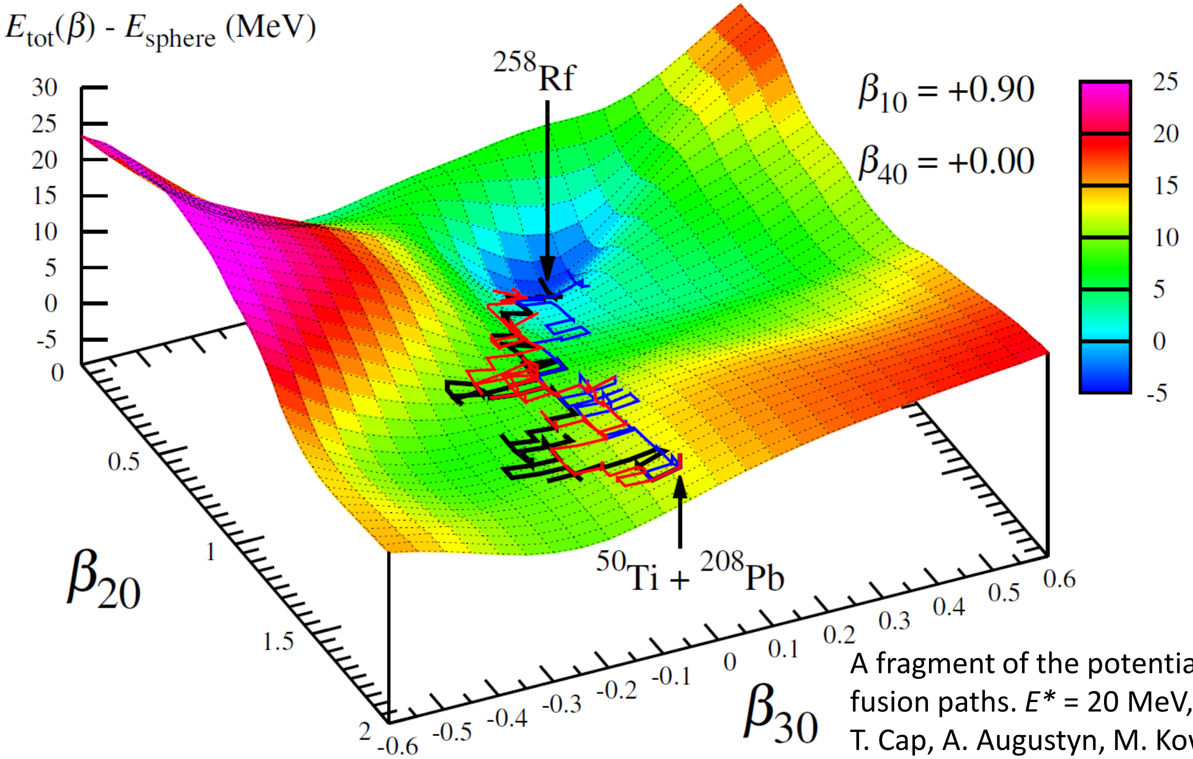

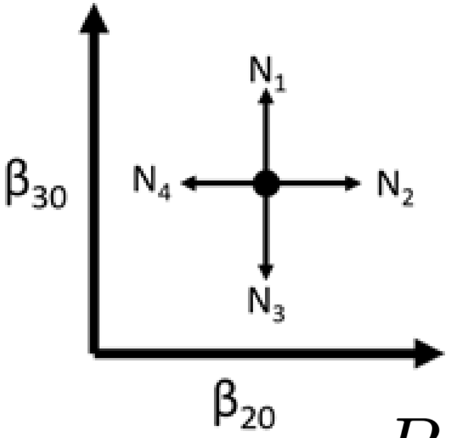

$$E_{rot} = l(l+1)\frac{(\hbar c)^2}{2I(\beta)}$$

$$P_{i\to j}(\ell) = \frac{N_j(\beta_j,\ell)}{\sum_{k=1}^{8} N_k(\beta_k,\ell)}$$

A fragment of the potential energy map for the ^{258}Rf nucleus calculated within the macroscopic-microscopic model with 3 fusion paths. E^* = 20 MeV, *l*=0ħ.
T. Cap, A. Augustyn, M. Kowal and K. Siwek-Wilczyńska, Phys. Rev. C **109**, L061603 (**2024**)

Biased, unconstrained random walk method

- The random walk occurs in a space where the dimensions β_{20}, β_{30}, and β_{40} are <u>unconstrained</u>, while $|\beta_{10}| < 1.6$.
- The random walk process continues until an end condition is met, either fusion or fission.
- Fusion is reached after crossing the saddle point ($\beta_{20} \leq 0.3$, $|\beta_{30}| \leq 0.2$, and $|\beta_{40}| \leq 0.2$). Splitting occurs when the neck radius is less than 2 fm.
- Reaching the end condition for a specific collision energy and angular momentum value defines a single evolution path.

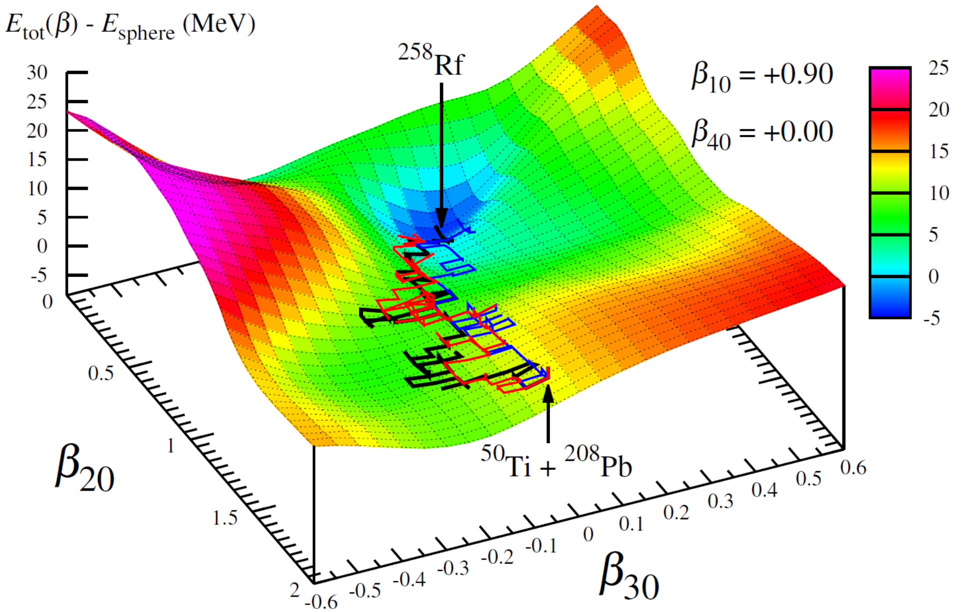

Example of a paths

$^{54}Cr + {}^{208}Pb$

$E^* = 50$ MeV, $l = 40$

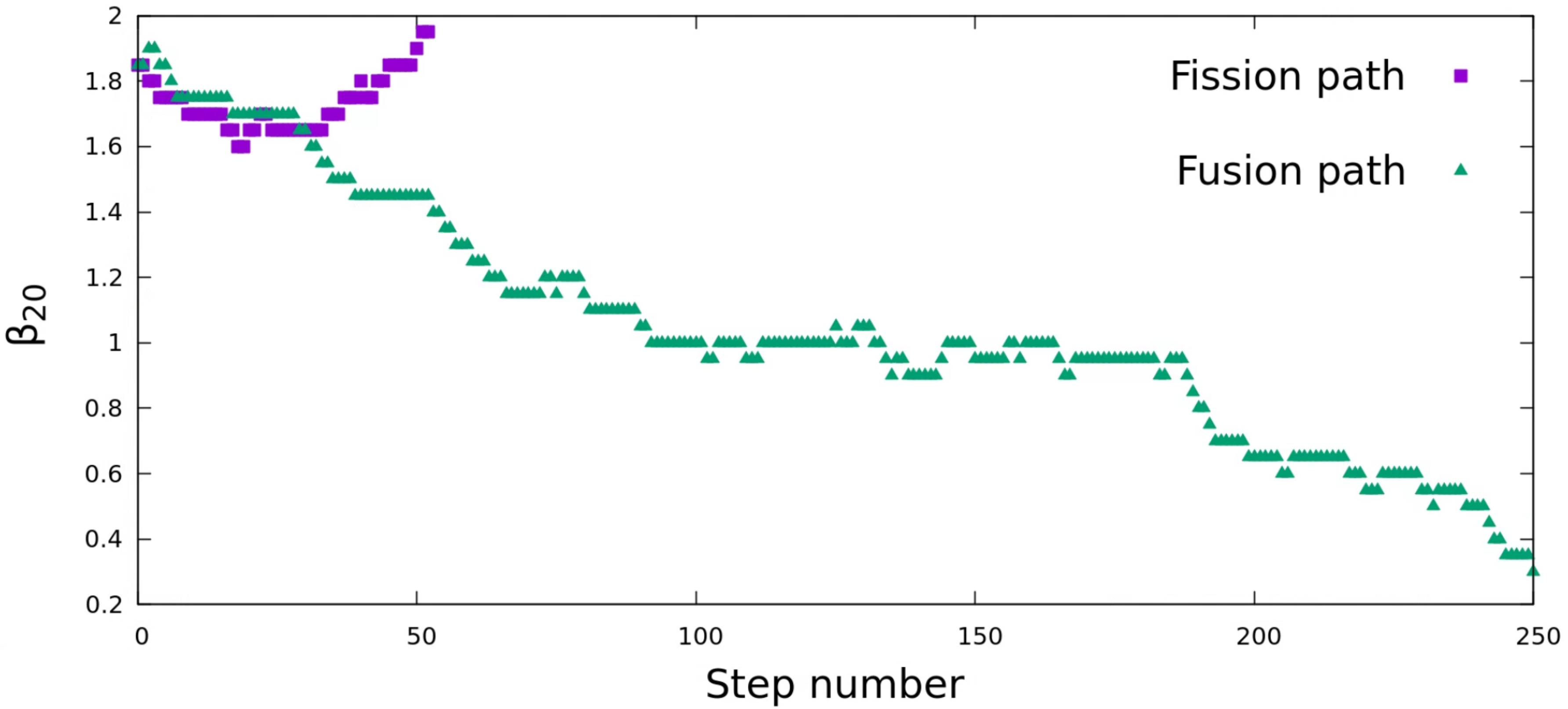

Example of a paths

$^{54}Cr + ^{208}Pb$

$E^* = 50$ MeV, $l = 40$

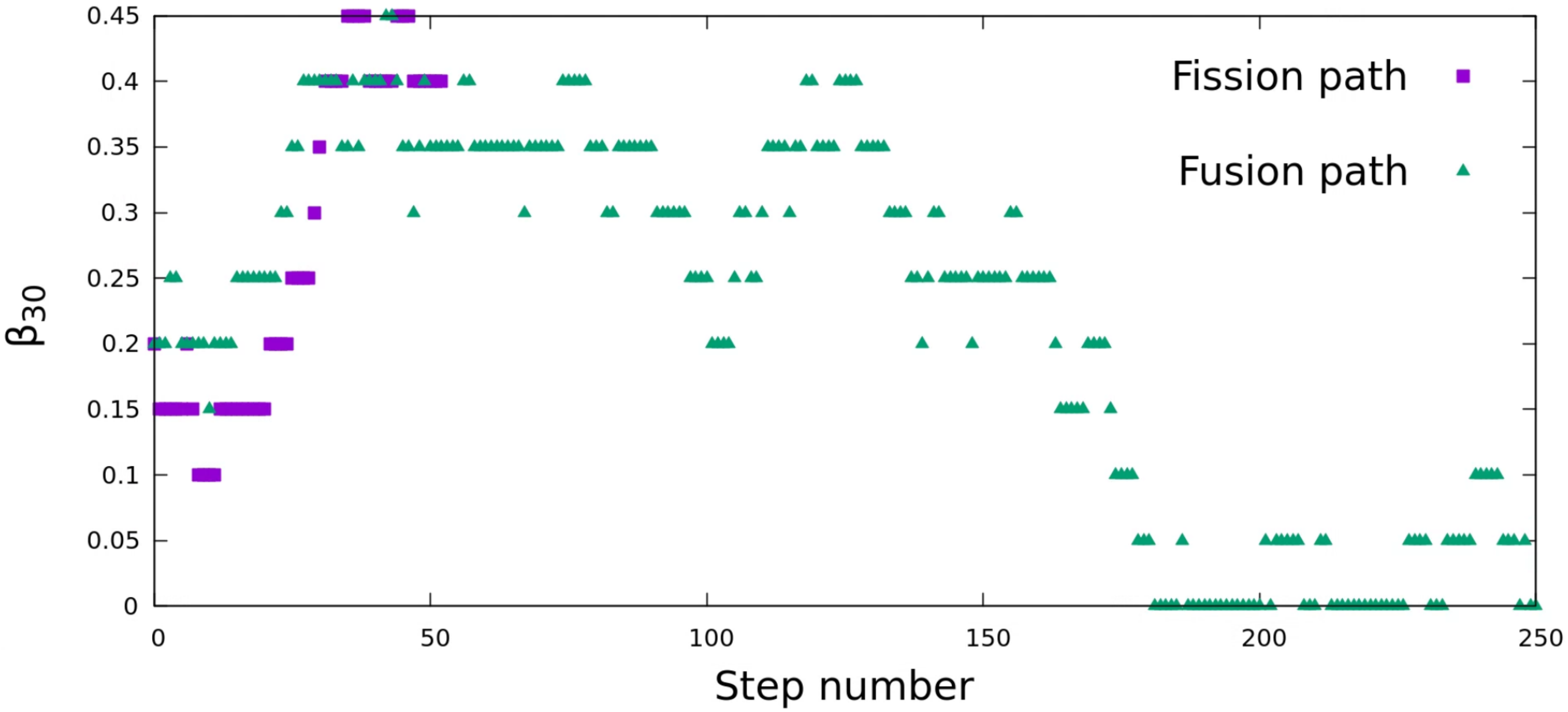

Example of a paths

$^{54}Cr + {}^{208}Pb$

$E^* = 50$ MeV, $l = 40$

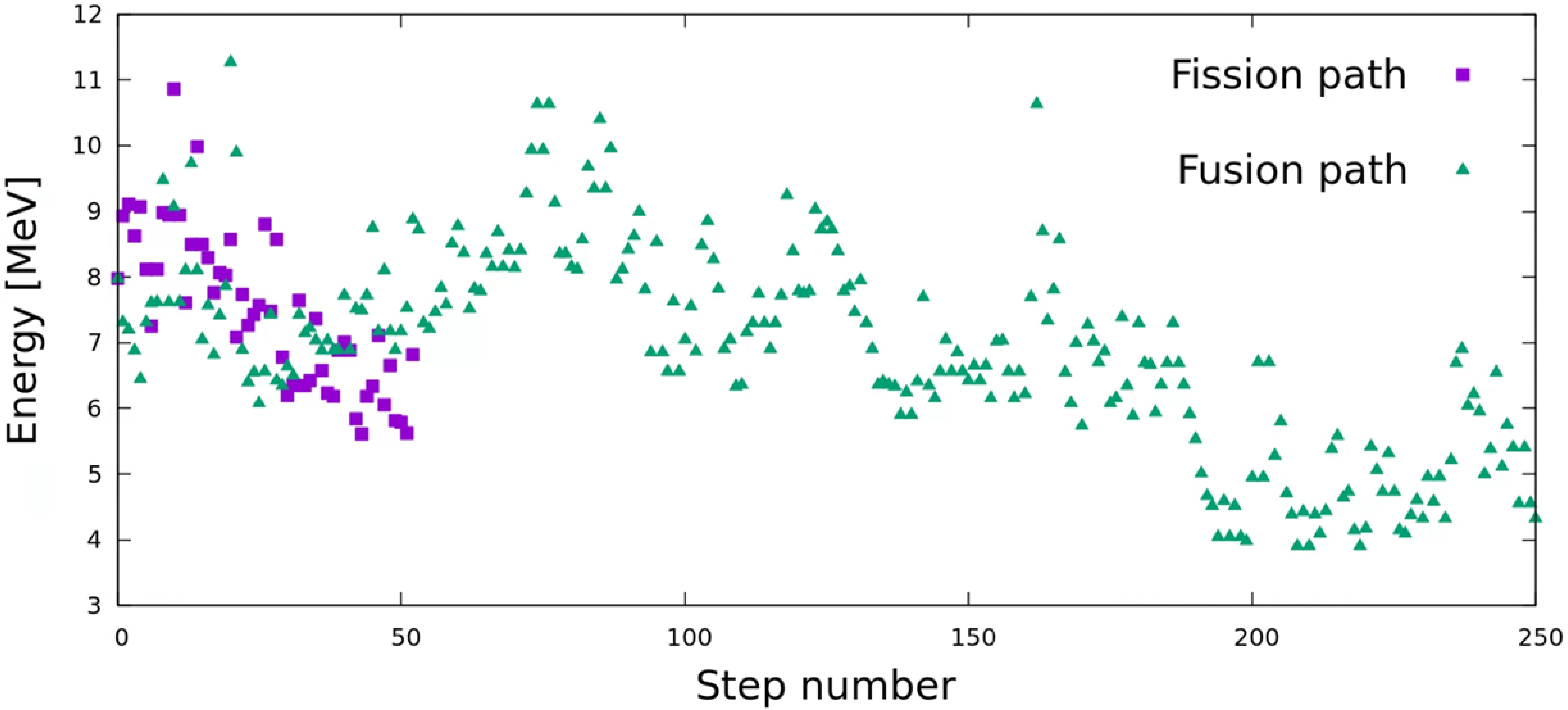

Example of a paths

$^{54}Cr + ^{208}Pb$

$E^* = 20$ MeV, $l = 0$

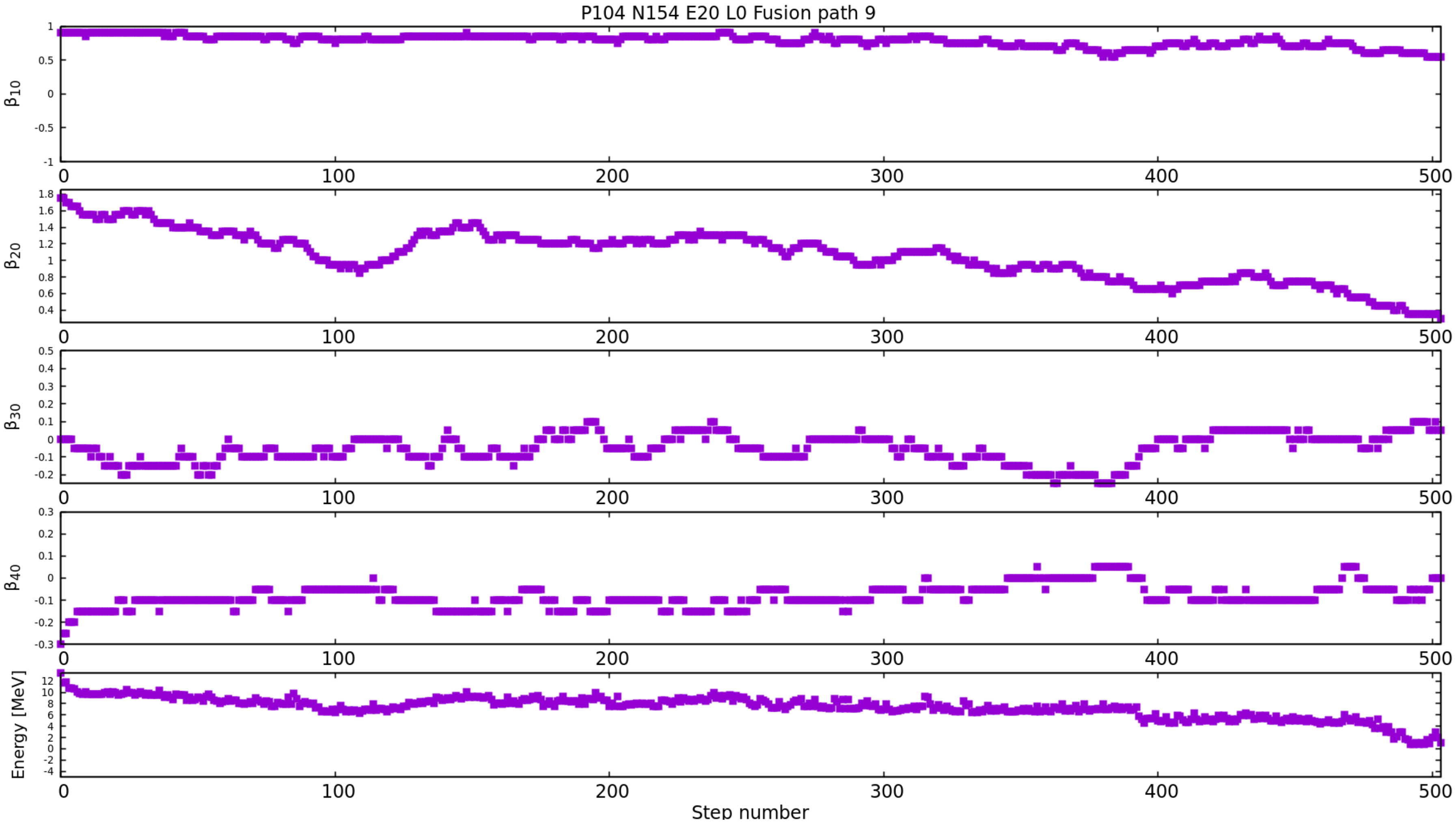

Biased, unconstrained random walk method

- Calculations were done for excitation energies from 15 to 70 MeV with 1 MeV step. 10^5 paths were calculated for a given energy and *l*-value from 0 to l_{max}. $P_{fus}(E_{cm}, l)$ is given as a ratio of the number of paths that lead to fusion to the total number of paths

$$P_{fus}(E_{cm}, l) = \frac{\text{paths which ended in fusion}}{10^5}$$

- ~ 3000 E^* and *l* combinations → ~300 million paths per system in the energy range

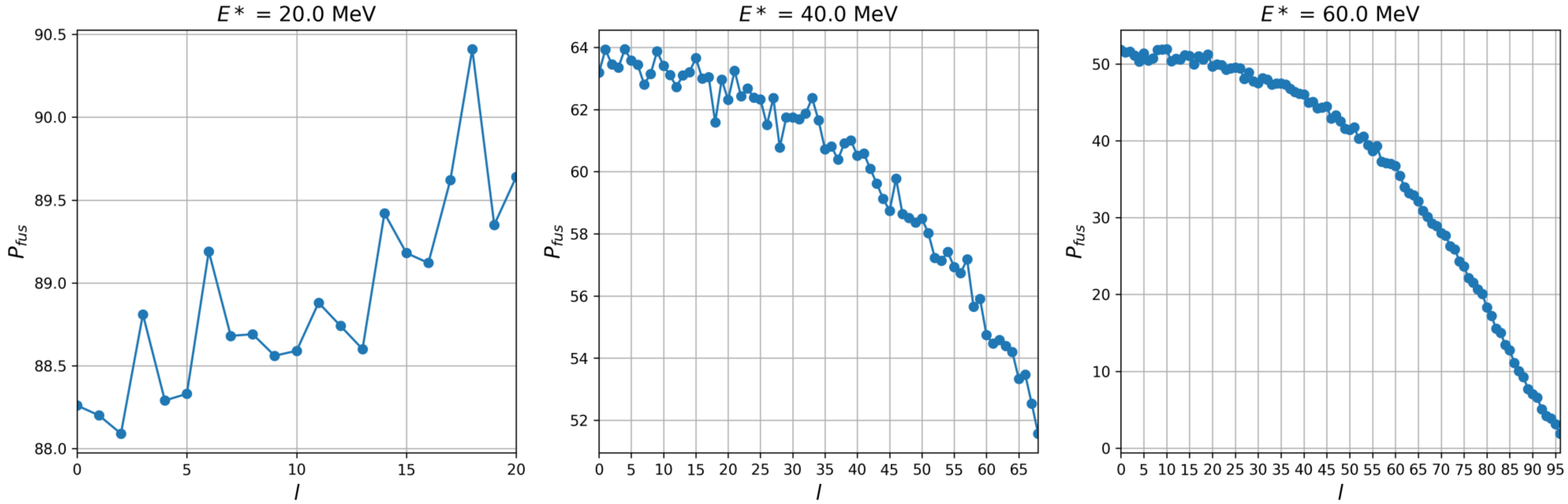

Plots of $P_{fus}(E_{cm}, l)$ for $^{48}Ca + ^{208}Pb$

Capture and fusion cross section

- Capture cross section and l_{max} calculated from FbD model
- Fusion cross section from the random walk method

$$\sigma_{fus} = \pi\lambda\!\!\!^{-}{}^2 \sum_{l=0}^{l_{max}} (2l+1)T(l)P_{fus}(l) = \sigma_{cap} \times P_{fus}$$

- Differential cross section distributions of $\frac{d\sigma_{cap}}{dl}$ (black) and $\frac{d\sigma_{fus}}{dl}$ (red) for ^{48}Ca+ ^{208}Pb:

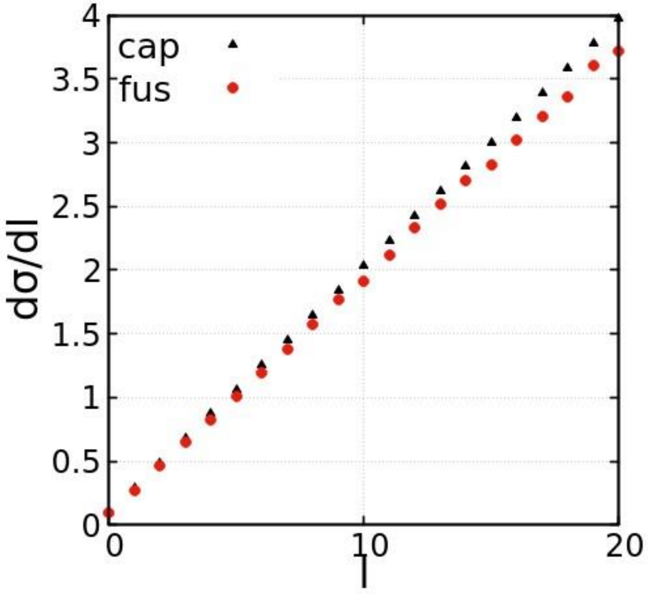

E* = 20 MeV

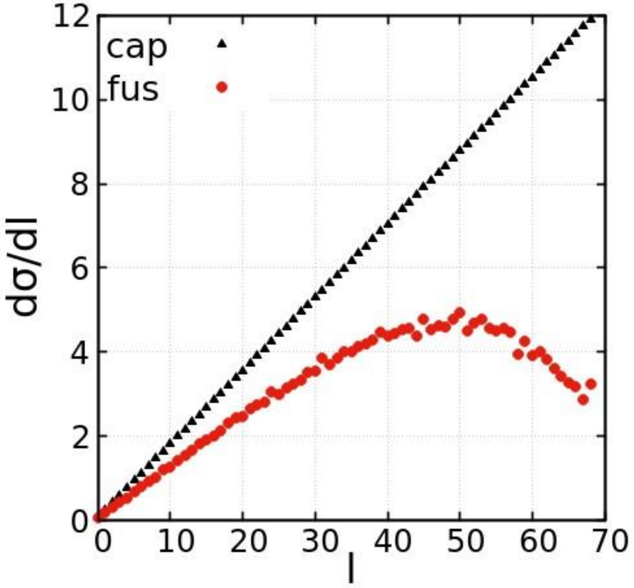

E* = 40 MeV

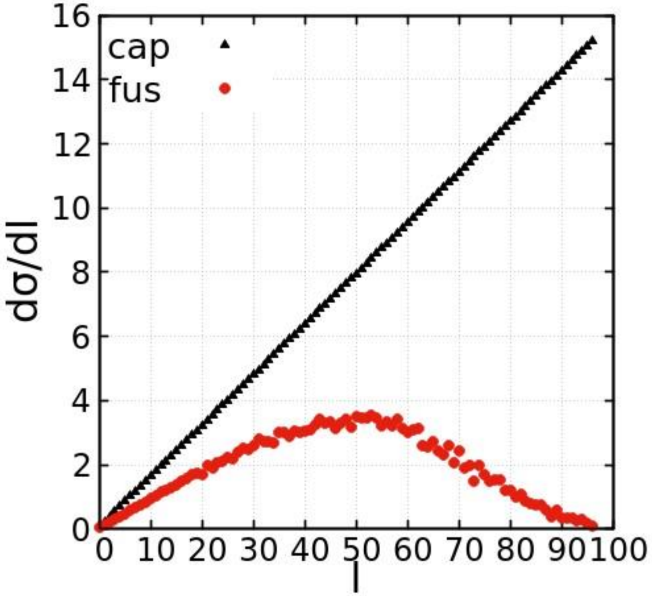

E* = 60 MeV

Fusion probability from the random walk

Average over l to get P_{fus} dependant on E_{cm}: $P_{fus}(E_{cm}) = \frac{\sum_{l=0}^{lmax}(2l+1)P_{fus}(l)}{(2l_{max}+1)^2}$ fusion probability averaged over l

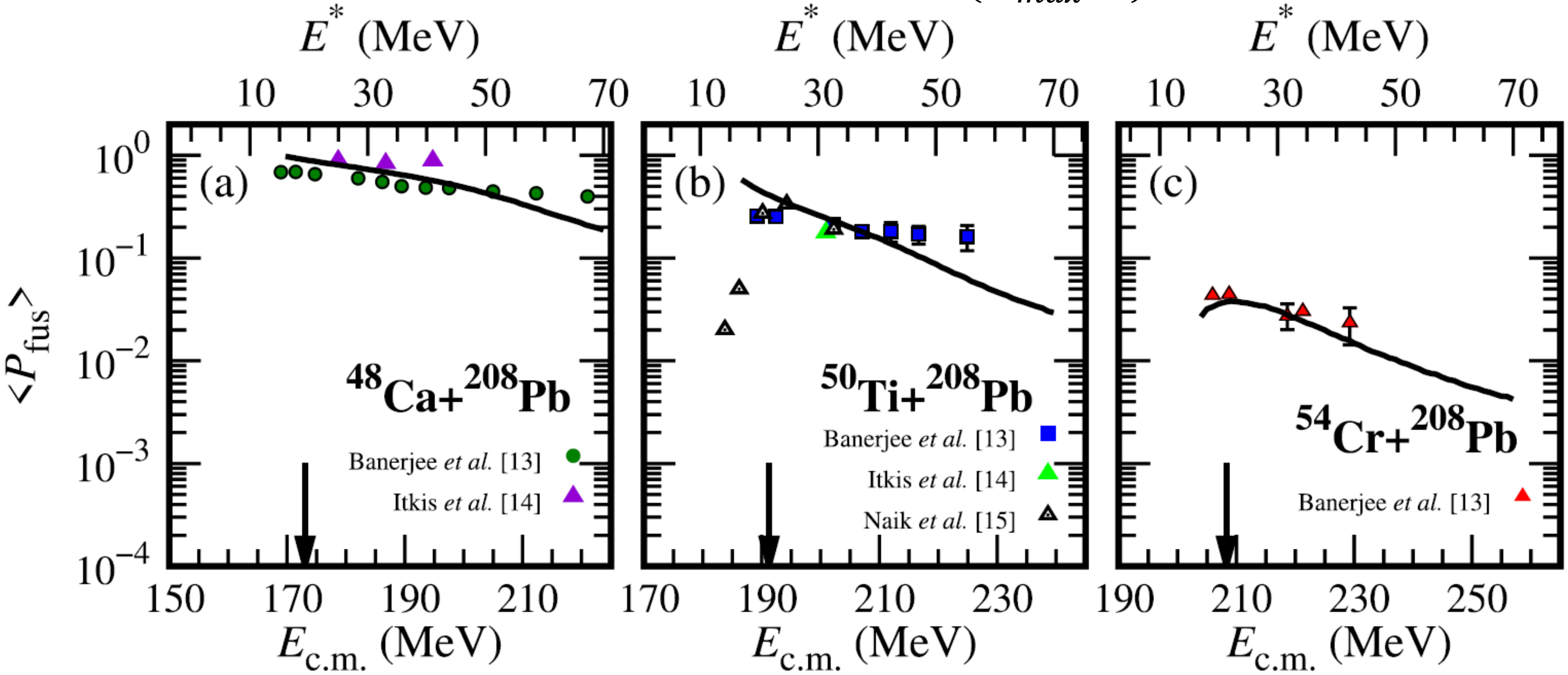

The averaged fusion probabilities < P_{fus} > (solid black lines) calculated using the random walk method for the ^{48}Ca+^{208}Pb, ^{50}Ti+^{208}Pb, and ^{54}Cr+^{208}Pb reactions. Experimental data are taken from [K. Banerjee et al., PRL 122, 232503 (2019)], [M. Itkis et al., EPJ 58, 178 (2022] and [R. S. Naik et al., PRC 76, 054604 (2007)] The arrows represent the locations of the mean entrance channel barrier B_0 for each reaction.

T. Cap, A. Augustyn, M. Kowal and K. Siwek-Wilczyńska,
Phys. Rev. C **109**, L061603 (**2024**)

NARODOWE CENTRUM BADAŃ JĄDROWYCH ŚWIERK

Results from another random walk model

- Model formulated in PhD thesis of M. Albertsson, (2021), "Nuclear fission and fusion in a random-walk model"
- Also recently published
- Different macro-micro energy model
- Three-quadratic-surface shape parametrization in 5 dimensional space
- Different approach to defining the start configuration and end conditions
- Similarly recreates the experimental data without fitting parameters of the fusion model
- Seems random walk method is a valid approach for fusion/fission probabilities of SHE

PHYSICAL REVIEW C **110**, 014624 (2024)

Formation of transfermium elements in reactions with ^{208}Pb

M. Albertsson,[1,2] B. G. Carlsson,[2] T. Døssing,[3] J. Randrup,[1] D. Rudolph,[4] and S. Åberg[2]

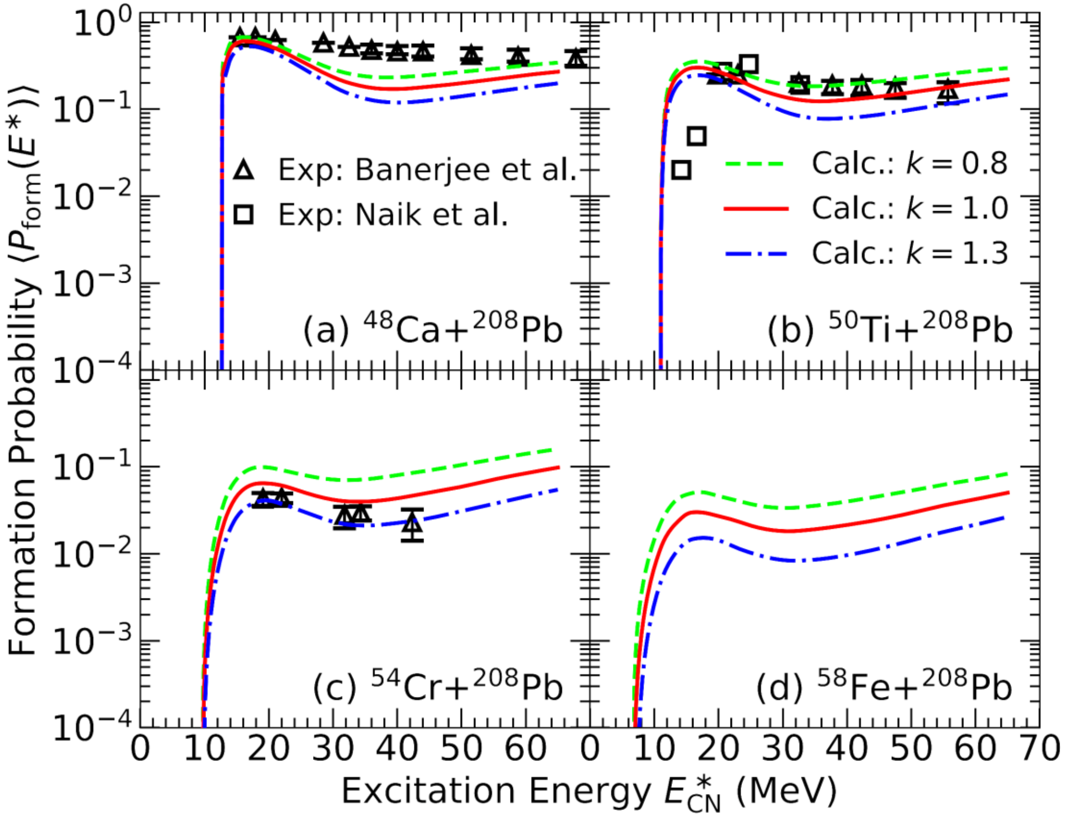

Calculated effective formation probability $<P_{form}(E^*_{CN})>$ as a function of the excitation energy E^*_{CN}, for three different dissipation strengths: k = 0.8 (green), 1.0 (red), and 1.3 (blue).

Refinements for the model

- Paper currently being prepared – “Hindrance Mechanism in Cold Fusion Reactions of Superheavy Elements”
- <u>Energy calculations and deformation space extended to 6 dimensions ($\beta_{10} - \beta_{60}$)</u>
- <u>Extend to the fusion-fission process</u>
- Extend to all even-even cold fusion systems and odd nuclei
- Test diffrent energy level density models
- Introduce shell correction damping
- Determine optimal step size for each β parameter
- Test multidimensional interpolation
- Allow for the emission of neutrons, protons and alfa particles during the random walk

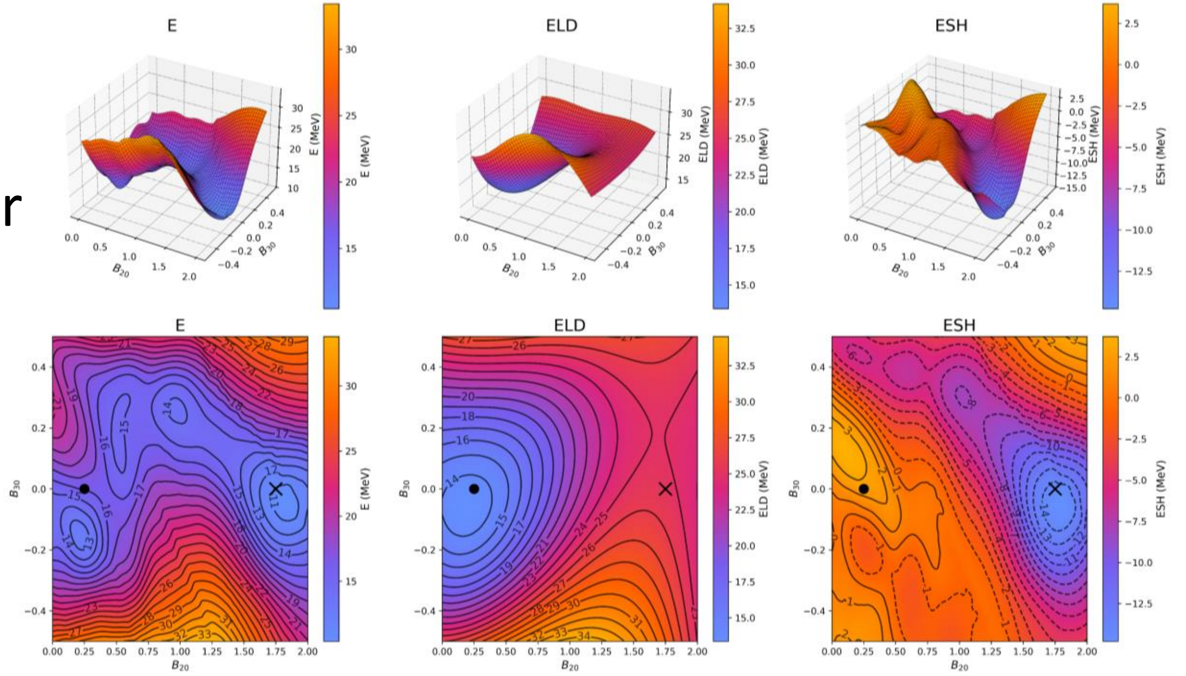

6D potential energy maps from the macro-micro model for the $^{48}Ca+^{208}Pb$ system. β_{10}, β_{40}, β_{50}, β_{60} as for the configuration. From the left: total energy, macroscopic energy, shell correction.

NARODOWE CENTRUM BADAŃ JĄDROWYCH ŚWIERK

Fusion-fission random walk in 6D

- The random walk always continues until the fission condition is met; events are categorized as:
  - DINE – if the system fissions without fulfilling any other condition, it's classified as deep inelastic collision/scattering
  - FAFI – if the system reaches β20 ≤ 1.4 but doesn't reach fusion, it's classified as fast fission
  - FUFI – if the system reaches fusion before under-going fission, it's classified as fusion-fission

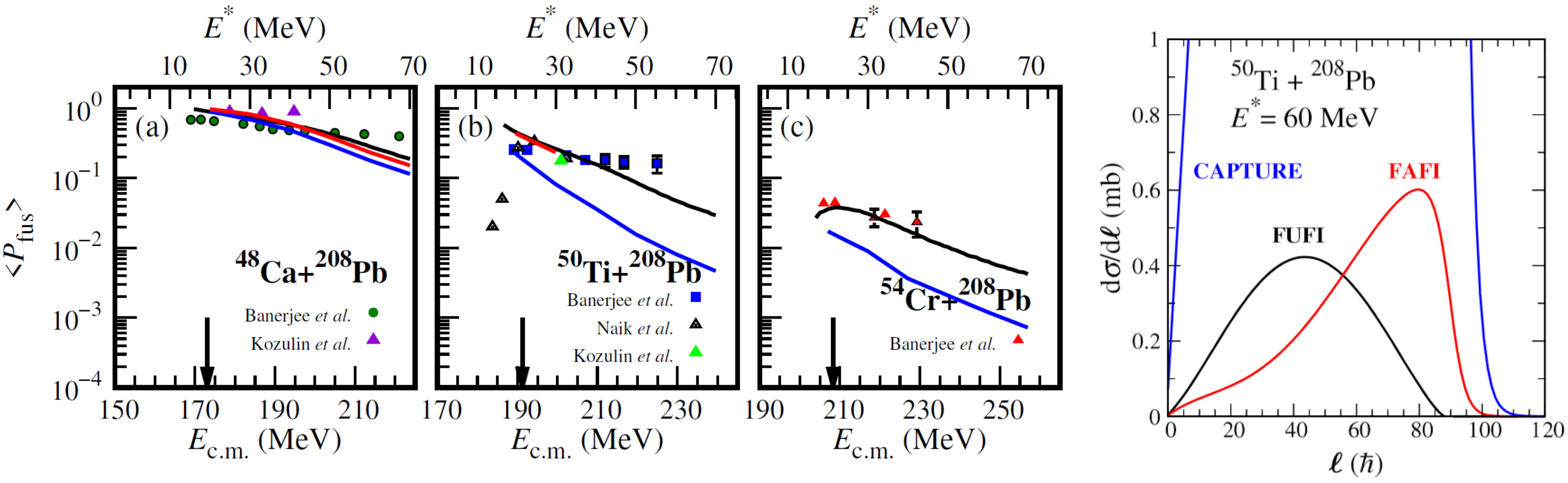

Fission condition (neck thickness) – 2fm, 1.75fm

Fission fragments mass distributions

- The final fission shapes can be divided, and their volumes compared, giving the mass distributions of fission fragments, for each E^* and *l*, which then can be averaged over *l*

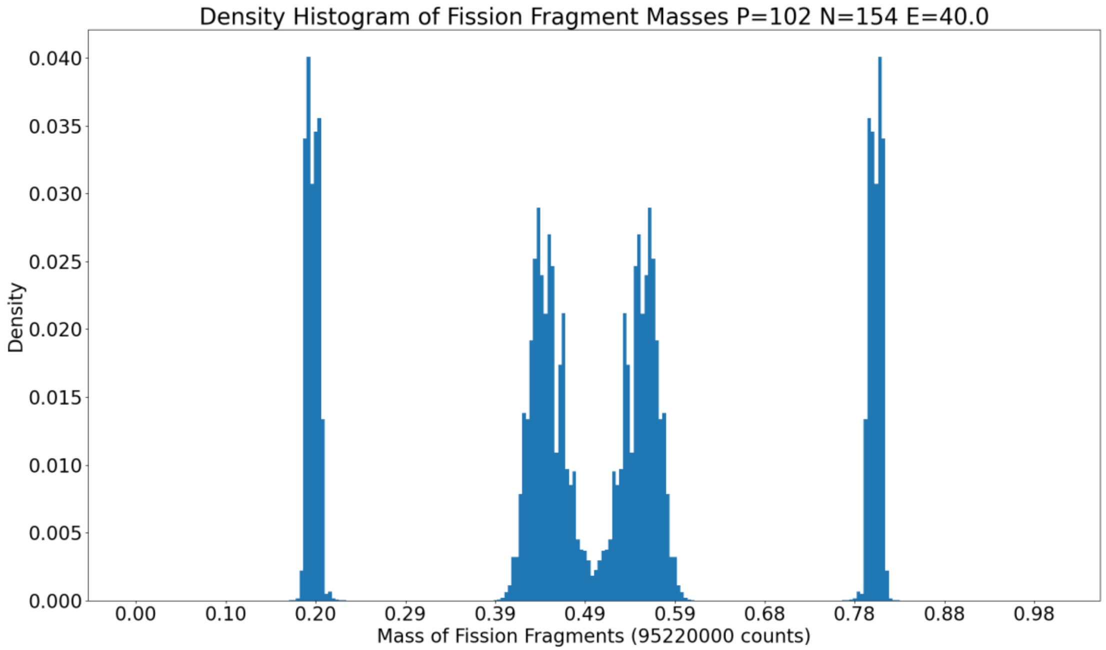

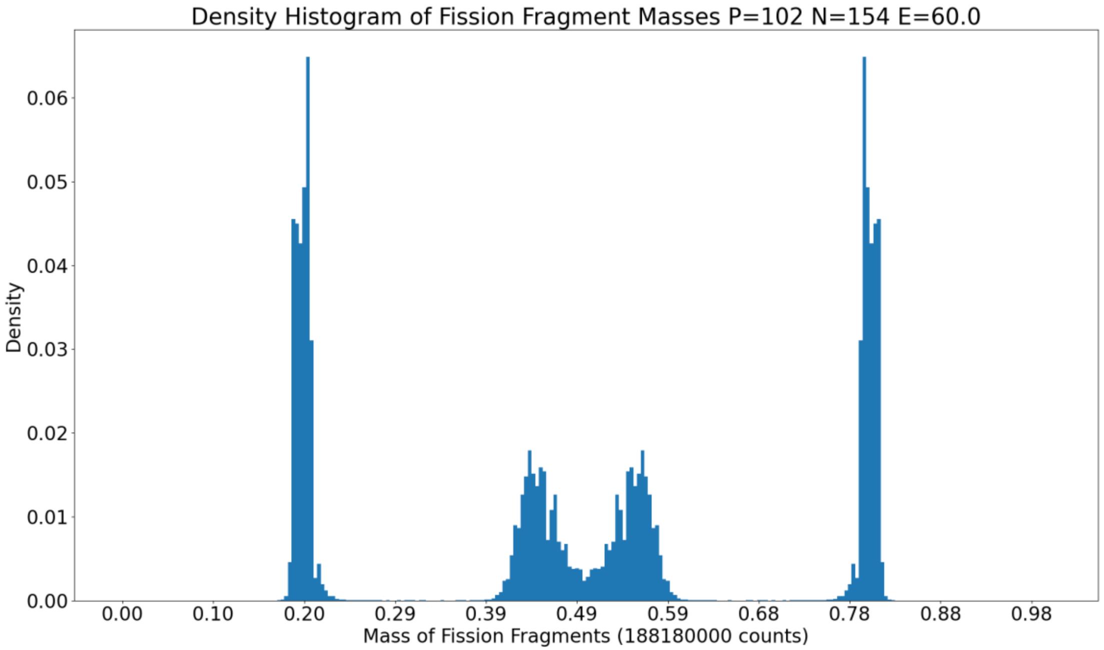

NARODOWE CENTRUM BADAŃ JĄDROWYCH ŚWIERK

Emission of neutrons, protons and alfa particles during the random walk

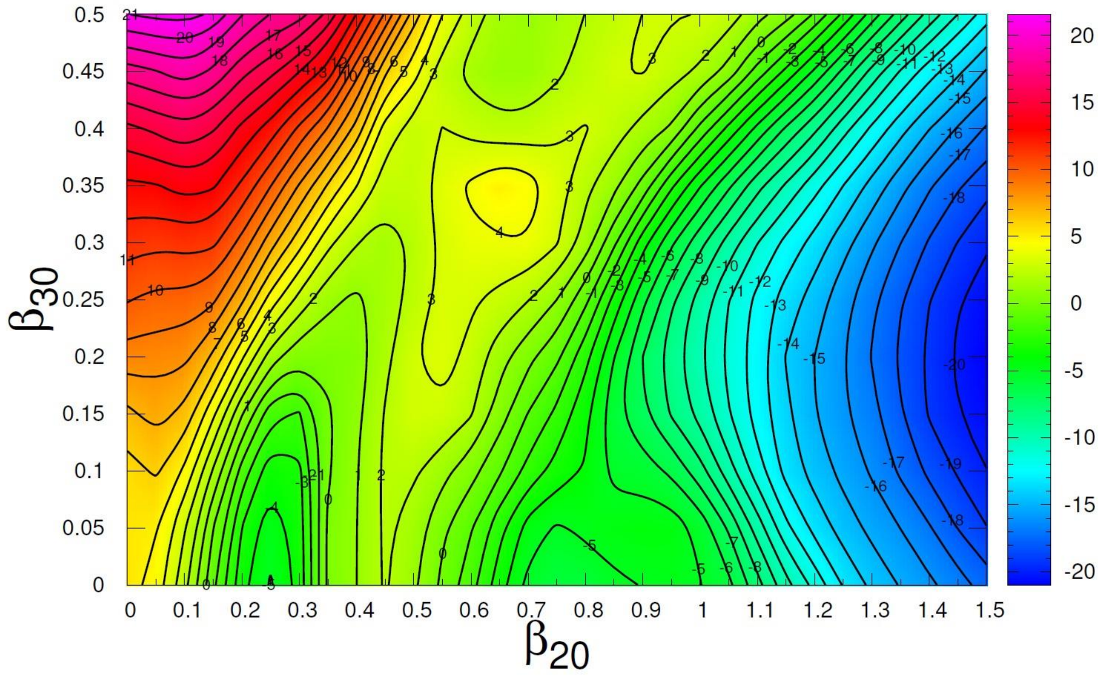

^{54}Cr+ ^{208}Pb, *I* = 0

-2 neutrons

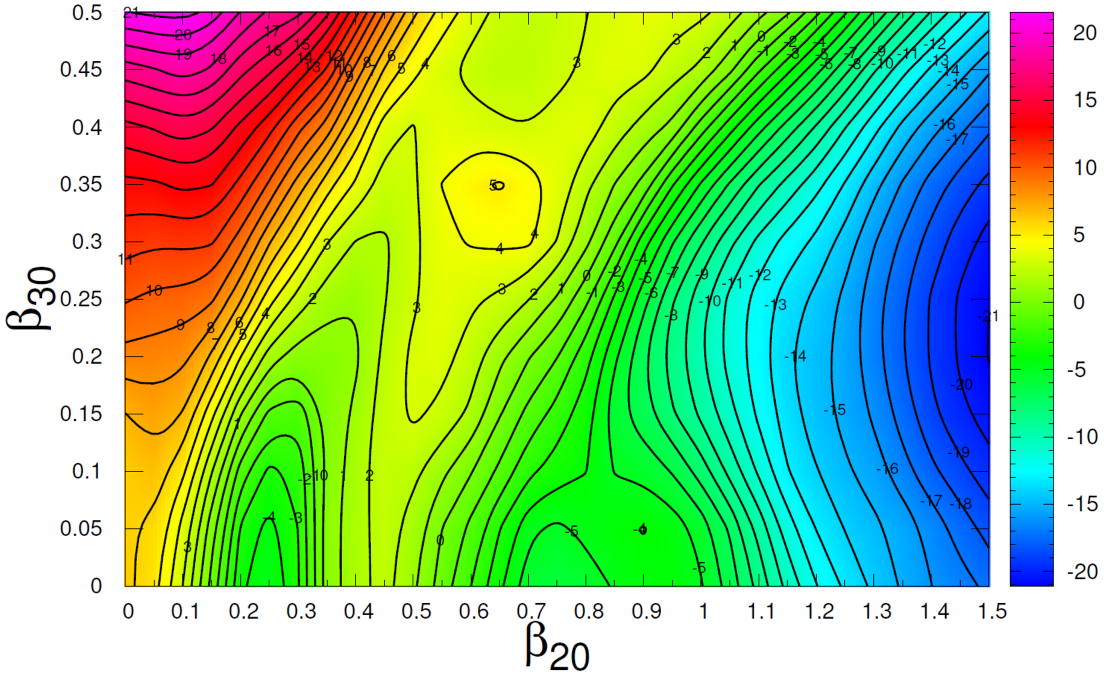

^{52}Cr+ ^{208}Pb, *I* = 0

Instead of moving only between shapes, we can also change the PESs.

Thank you for your attention !

NATIONAL CENTRE FOR NUCLEAR RESEARCH ŚWIERK

www.ncbj.gov.pl

BONUS SLIDES

Summary

- The random walk method reproduces experimental results for probability of fusion, even though there are no fitted parameters within the model itself
- Including the β_{10} as an actual shape variable allowed to describe the starting point configuration with only 4 deformation parameters
- The new approach makes possible to predict mass fragment distributions, which can be compared with experimental data
- The random walk method looks to be a promising direction of study, both for fusion and fission of superheavy nuclei

Touching spheres

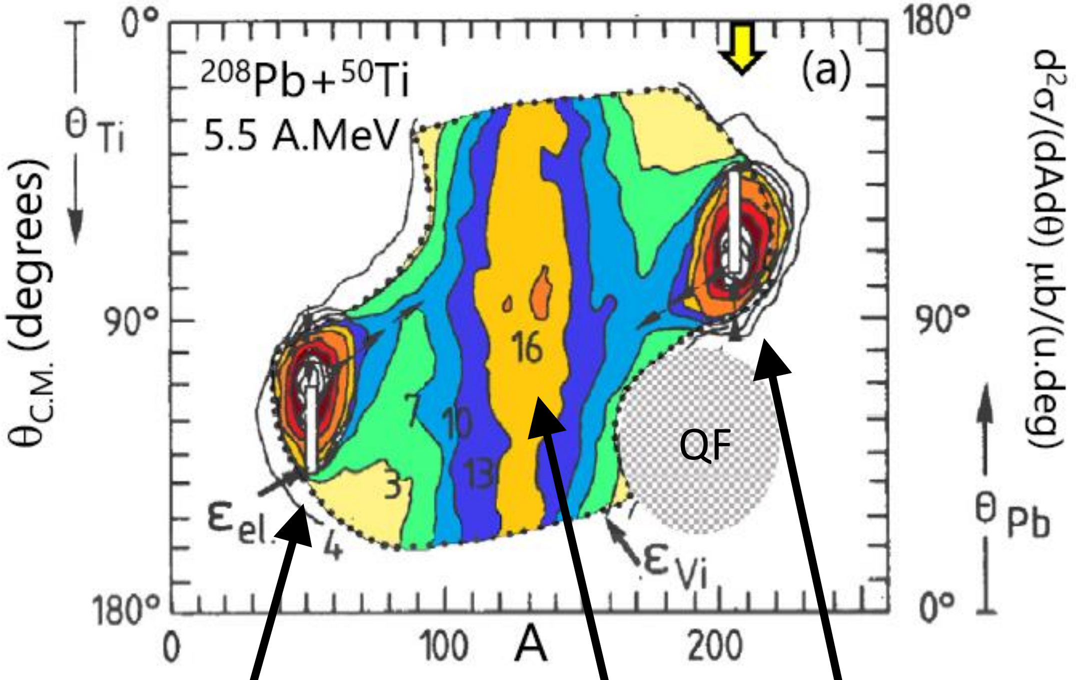

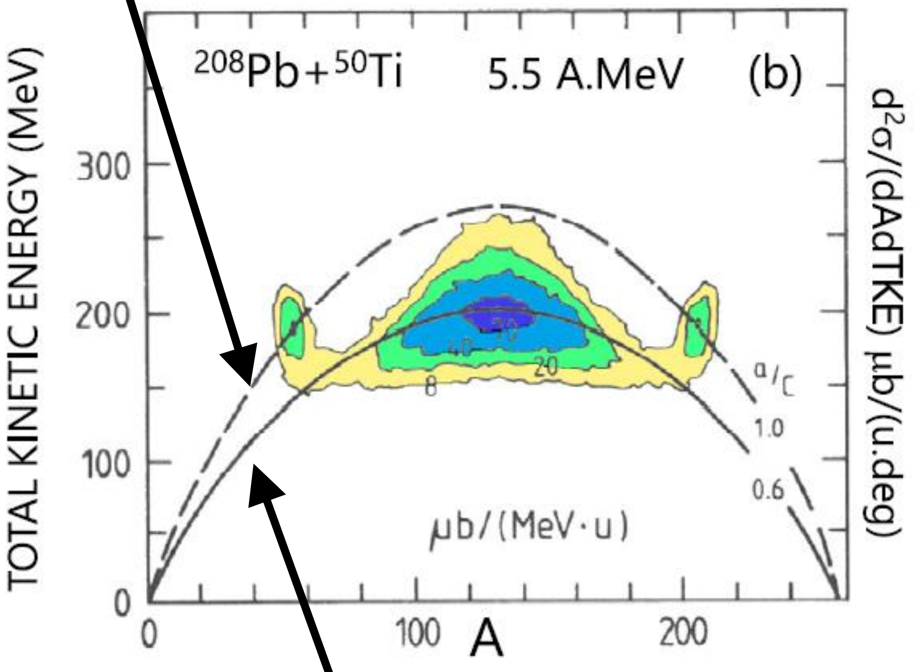

50Ti

Fusion
Fission

208Pb

Fully damaped collisions
Viola systematics

R. Bock et al., Nuclear Phys. A 388 (1982) 334–380

Ec.m. = 222 MeV, *B0* = 190 MeV, *E** = 50 MeV

R. Bock et al., Nuclear Phys. A 388 (1982) 334–380

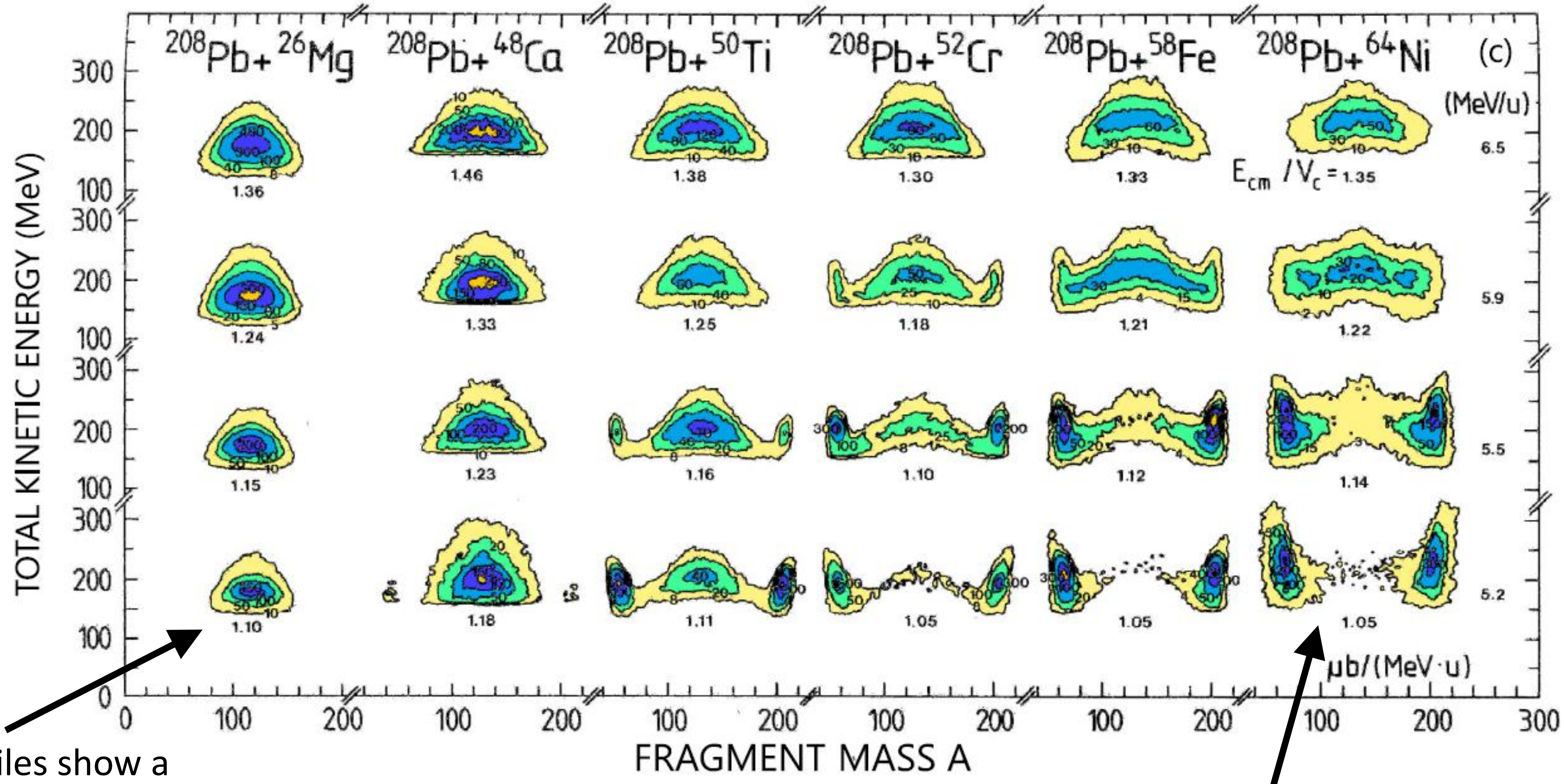

The lighter projectiles show a symmetric-peaked mass distribution of binary events at all energies, whose width increases with beam energy

For the heavy systems the symmetric yield is only prominent at the highest energies, and at low energies mass-asymmetric events predominate

⇒ small *Pfus* at lower bombarding energies

⇒ cold fusion reactions are below *B0*

Itkis et al., Eur. Phys. J. A (2022) 58:178

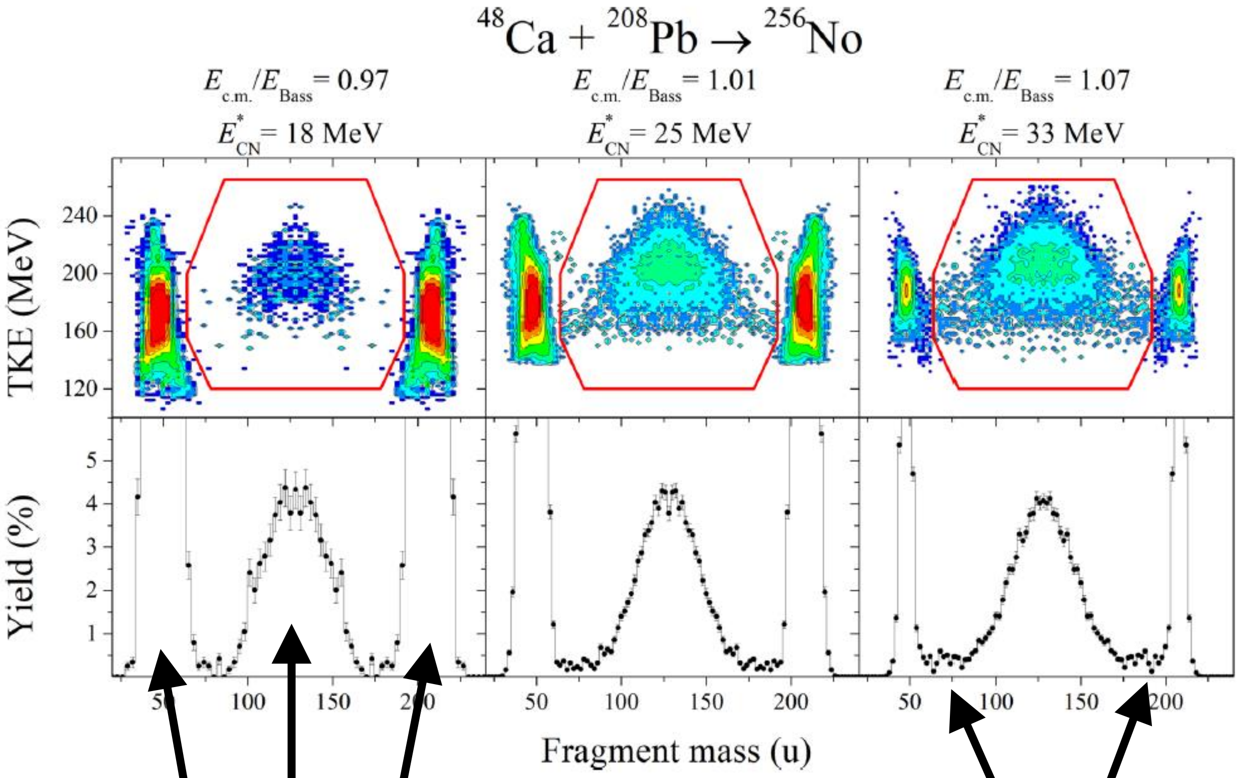

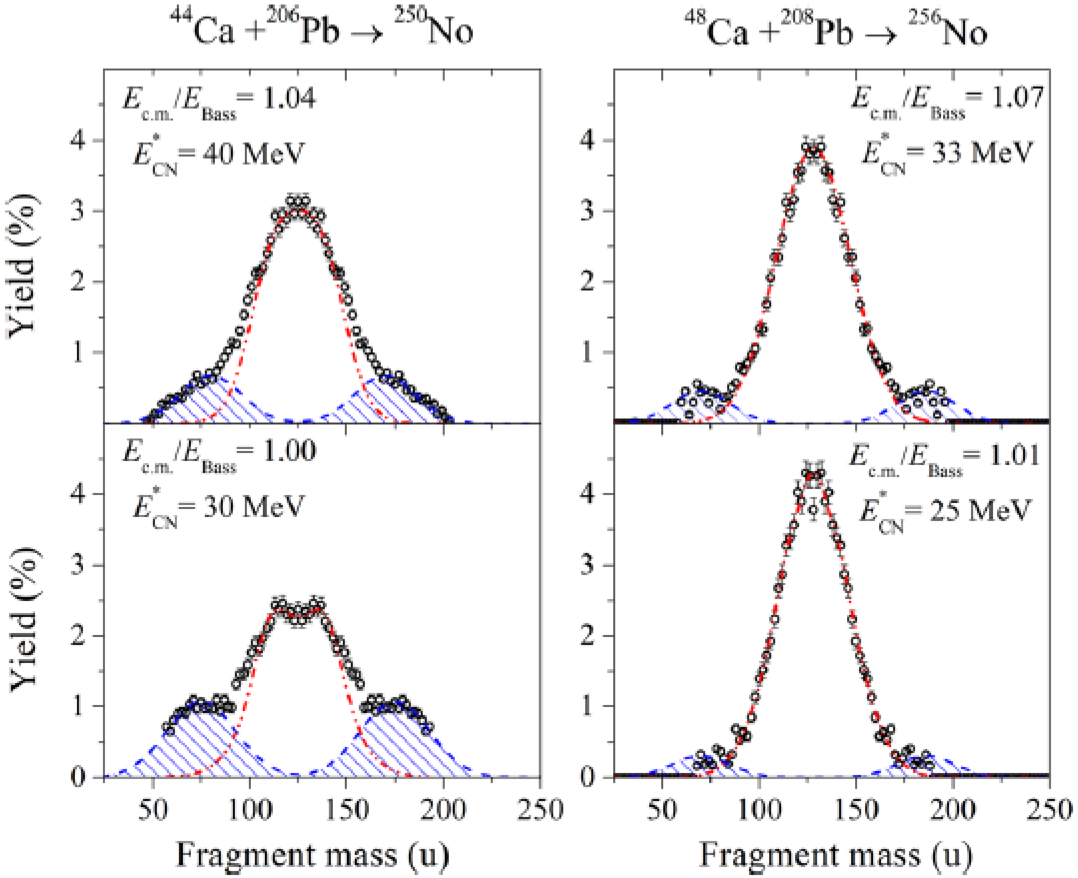

Fusion-Fision

QF – not fully included in Bock's measurements due to detection efficiency

E, QE, DIC increase when we go down with beam energy

Rotational energy E_{rot}

- Rigid body approximation
- Moment of inertia calculated analytically

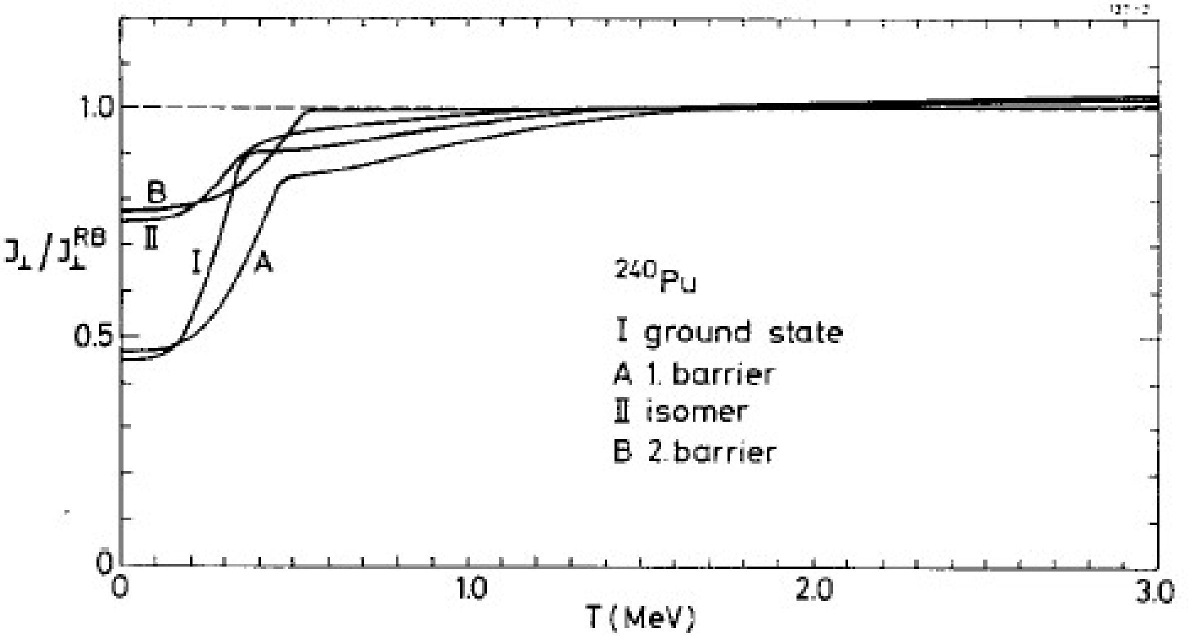

M. Brack, T. Ledergerber, H. Pauli, A. Jensen, Nuclear Physics A **234**, 185–215 (1974)

$$E_{rot} = l(l+1)\frac{(\hbar c)^2}{2I(\beta)} \qquad \mathbf{I} = \begin{pmatrix} I_\perp & & \\ & I_\perp & \\ & & I_\parallel \end{pmatrix}$$

$$I_\perp = \frac{1}{5}\rho R_0{}^5 \int \sin(\theta)(\pi\sin^2(\theta) + 2\pi\cos^2(\theta))(1 + \frac{1}{2}\sqrt{\frac{3}{\pi}}\beta_{10}\cos(\theta) + \frac{1}{4}\sqrt{\frac{5}{\pi}}\beta_{20}(3\cos^2(\theta) - 1)$$
$$+ \frac{1}{4}\sqrt{\frac{7}{\pi}}\beta_{30}(5\cos^3(\theta) - 3\cos(\theta)) + \frac{1}{16}\sqrt{\frac{9}{\pi}}\beta_{40}(35\cos^4(\theta) - 30\cos^2(\theta) + 3))^5 d\theta$$

Macroscopic energy E_{mac}

$$E_{mac}(Z,N,\beta) = -a_v(1-\kappa_v I^2)A + a_s(1-\kappa_s I^2)A^{2/3}B_S(\beta) + a_0 A^0 + c_1 Z^2 A^{-1/3} B_C(\beta) - c_4 Z^{4/3} A^{-1/3} - f(k_F r_p) Z^2 A^{-1} + \bar{\Delta}_{mac}$$

- Liquid drop model
- Responsible for the majority of energy/mass
- Dependence on shape in the surface and Coulomb term
- Most often normalized with respect to the sphere

$$B_S = \frac{A^{-2/3}}{8\pi^2 r_0^2 a^4} \int\int_V \left(2 - \frac{r_{12}}{a}\right) \frac{e^{-r_{12}/a}}{r_{12}/a} d^3 r_1 d^3 r_2,$$

$$E_{mac}^{gs} = E_{mac}^{gs}(deformation) - E_{mac}^{gs}(sphere)$$

$$B_C = \frac{15}{32\pi^2} \frac{A^{-5/3}}{r_0^5} \int\int_V \frac{1}{r_{12}} \left[1 - \left(1 + \frac{1}{2}\frac{r_{12}}{a_{den}}\right) e^{-r_{12}/a_{den}}\right] d^3 r_1 d^3 r_2$$

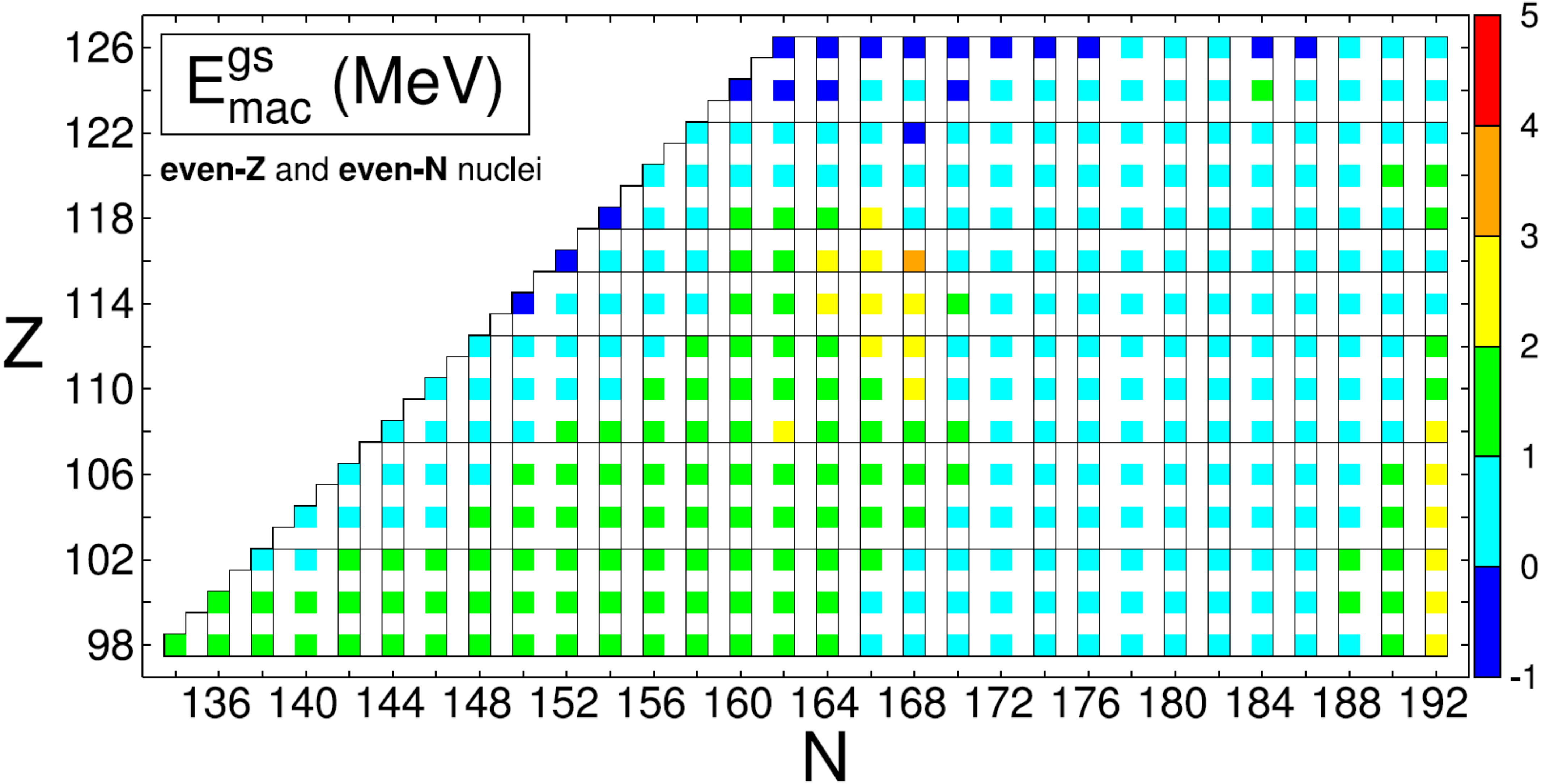

P. Jachimowicz, M. Kowal, J. Skalski, Properties of heaviest nuclei with 98≤Z≤126 and 134≤N≤192, Atomic Data and Nuclear Data Tables, Volume 138, 2021, 101393

Microscopic energy E_{mic}

$$E_{mic}(Z,N,\beta) \quad = \quad E^{sh}_{corr}(Z,N,\beta) + E^{pair}_{corr}(Z,N,\beta)$$

- Strutinsky shell correction based on the deformed Woods–Saxon single-particle potential

$$V_{WS}(\vec{r}) = -\frac{V}{1 + e^{d(\vec{r},\beta)/a_{ws}}}$$

- The single-particle potential is diagonalized in the deformed harmonic-oscillator basis
- Pairing energy, pair correlation from Bardeen–Cooper–Schrieffer (BCS) theory

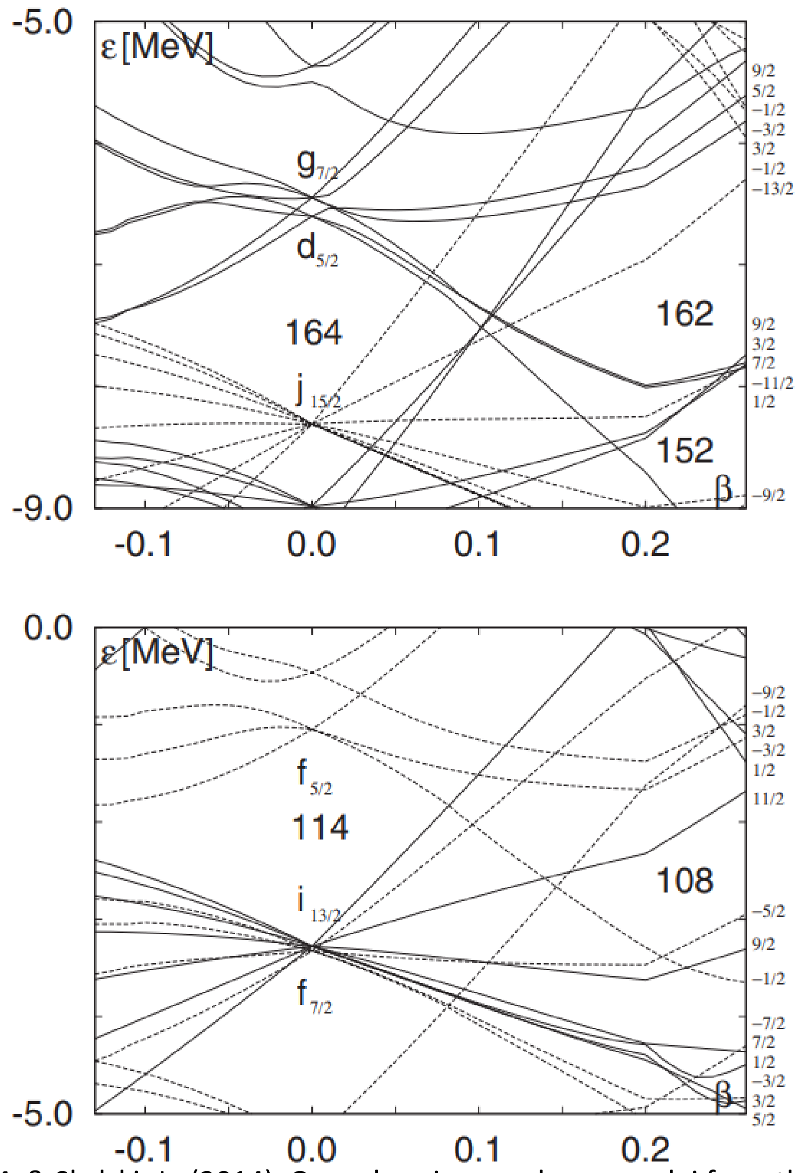

Jachimowicz, P. & Kowal, M. & Skalski, J.. (2014). Q α values in superheavy nuclei from the deformed Woods-Saxon model. Physical Review C. 89. 10.1103/PhysRevC.89.024304.

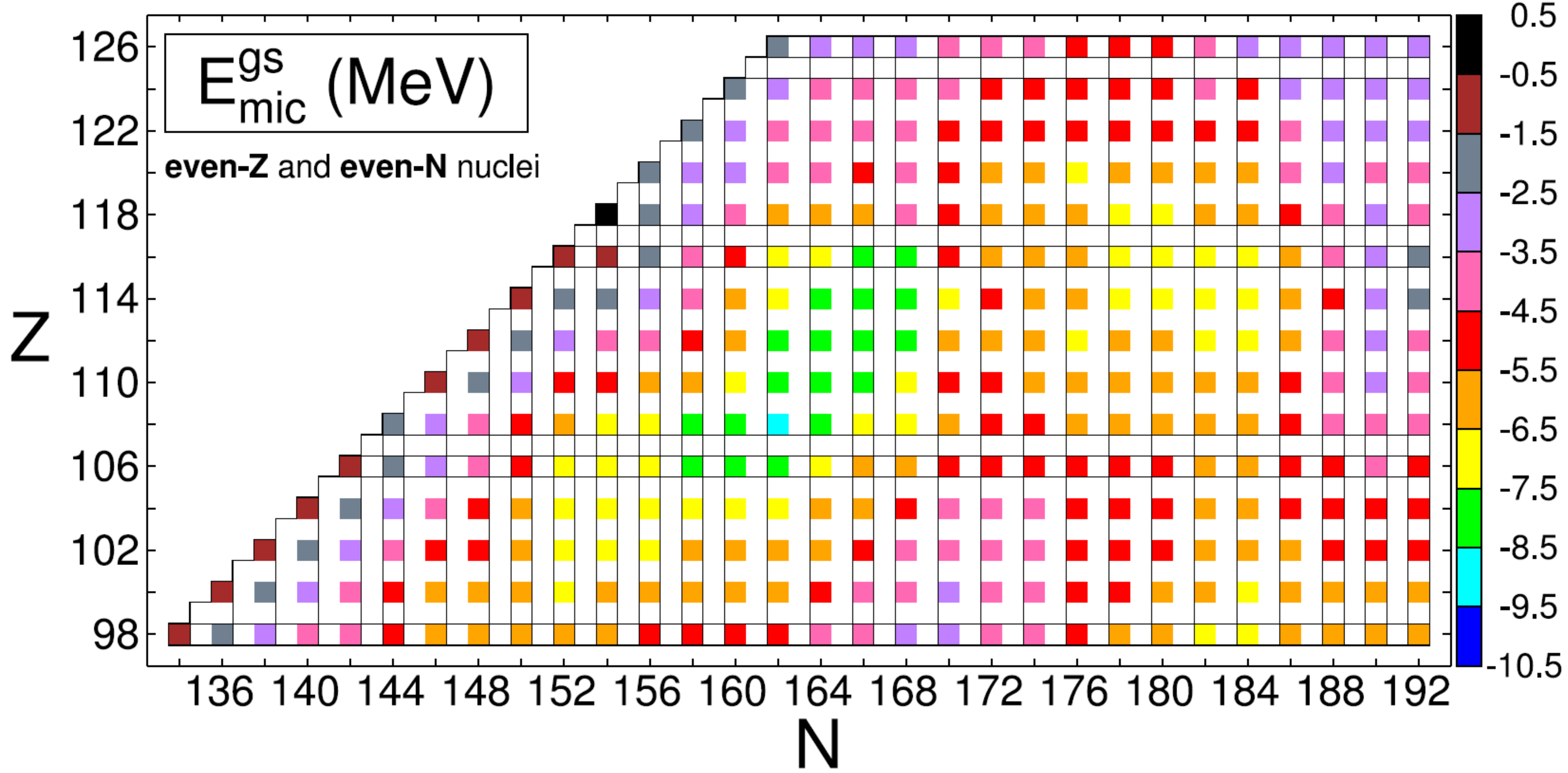

P. Jachimowicz, M. Kowal, J. Skalski, Properties of heaviest nuclei with 98≤Z≤126 and 134≤N≤192, Atomic Data and Nuclear Data Tables, Volume 138, 2021, 101393

In the **FBD** model, we use
1D motion approximation

The system must overcome an internal barrier ***H*** to fuse.

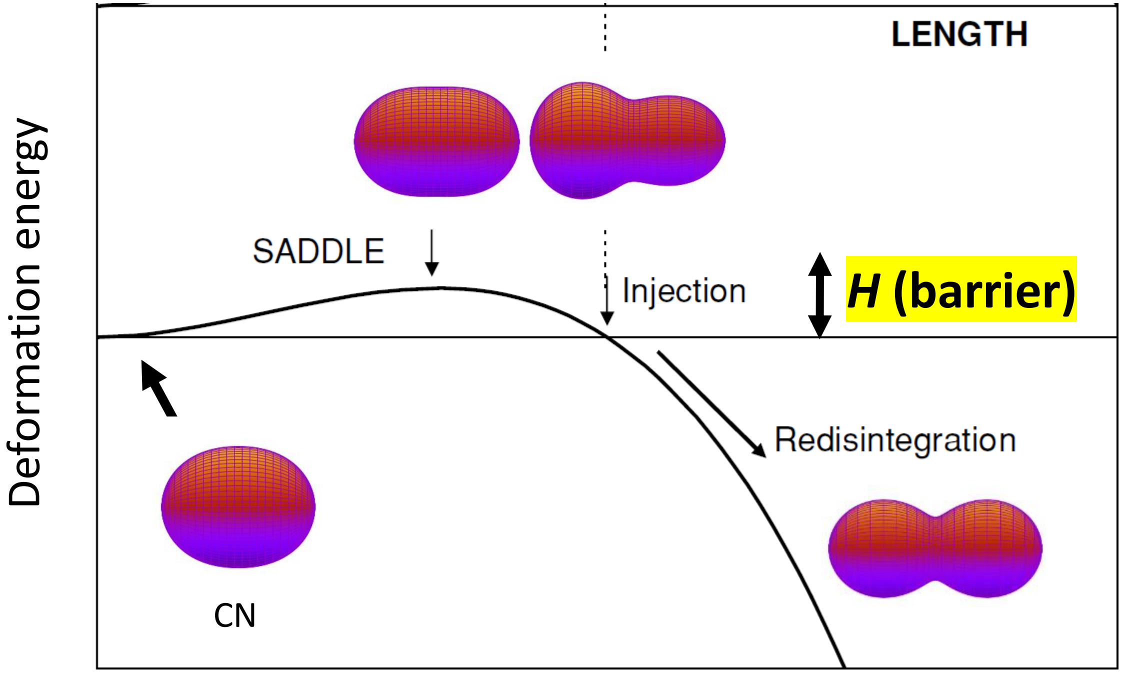

L is the effective elongation (along the fusion path)

Macroscopic deformation energies are calculated using the parameterization of the nuclear shapes by two spheres joined smoothly by a third quadratic surface of revolution.

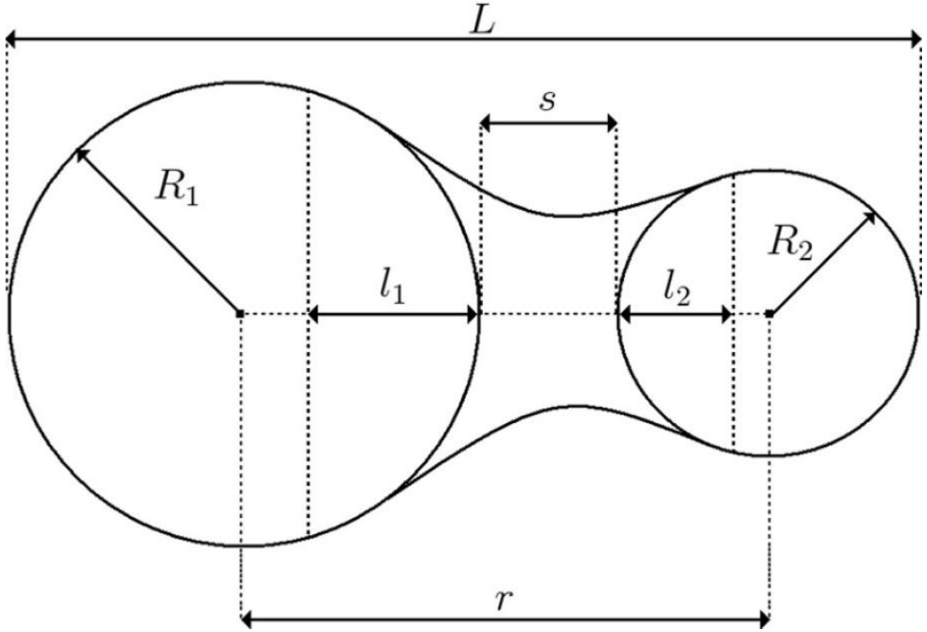

The distance between the nuclear surfaces of two colliding nuclei at the **injection point** s_{inj} is the only adjustable parameter of the model.

s_{inj} distance was parametrized
by analyzing 27 cold fusion reactions.

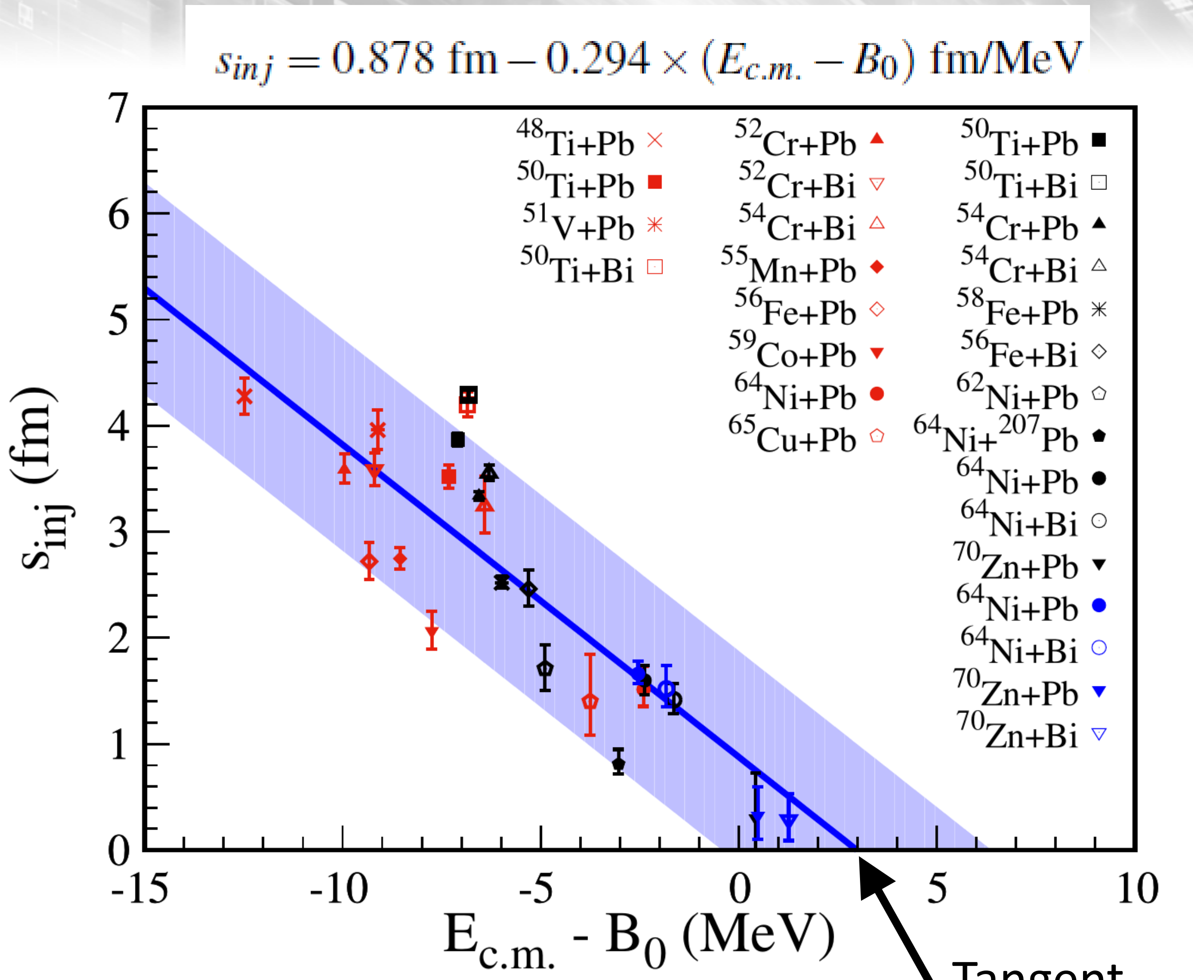

Tangent configuration

Energy relative to the entrance channel barrier B_0

Macroscopic deformation energies are calculated using the parameterization of the nuclear shapes by two spheres joined smoothly by a third quadratic surface of revolution.

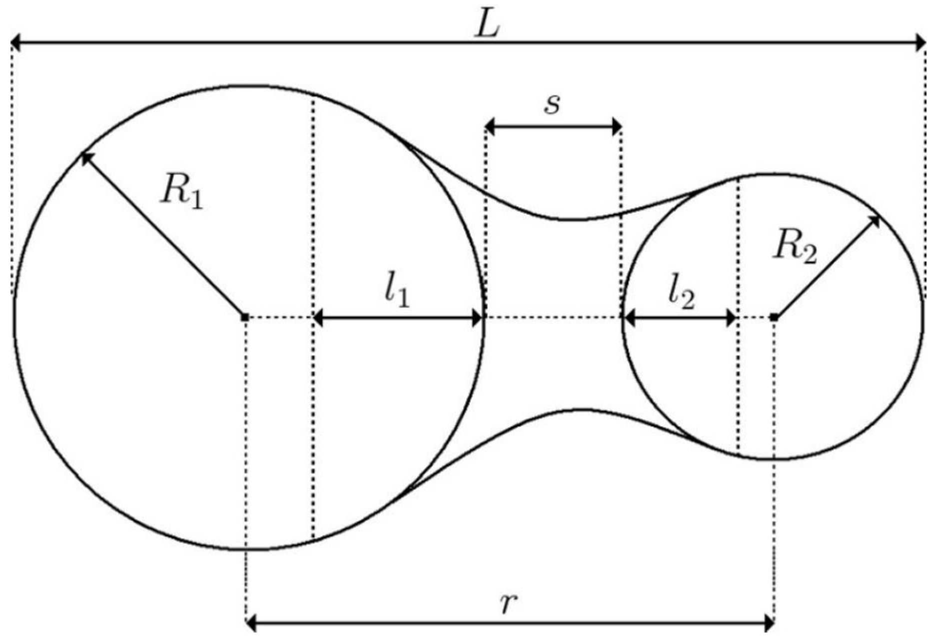

The distance between the nuclear surfaces of two colliding nuclei at the **injection point** s_{inj} is the only adjustable parameter of the model.

s_{inj} distance was parametrized by analyzing 27 cold fusion reactions.

Fusion probability averaged over l

$$P_{fus}(E_{c.m.}) = \frac{\sum_{l=0}^{lmax}(2l+1)P_{fus}(l)}{(2l_{max}+1)^2}$$

Below *B0*, the *Pfus* growth comes from the reduction in the height of the internal barrier opposing fusion.

$s_{injection}$ > 0 fm

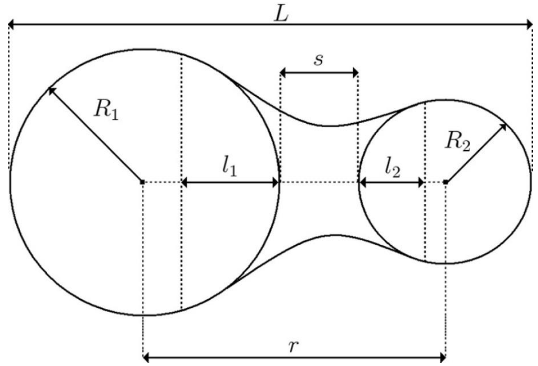

Tangent configuration of projectile and target ($s_{injection}$ = 0 fm)

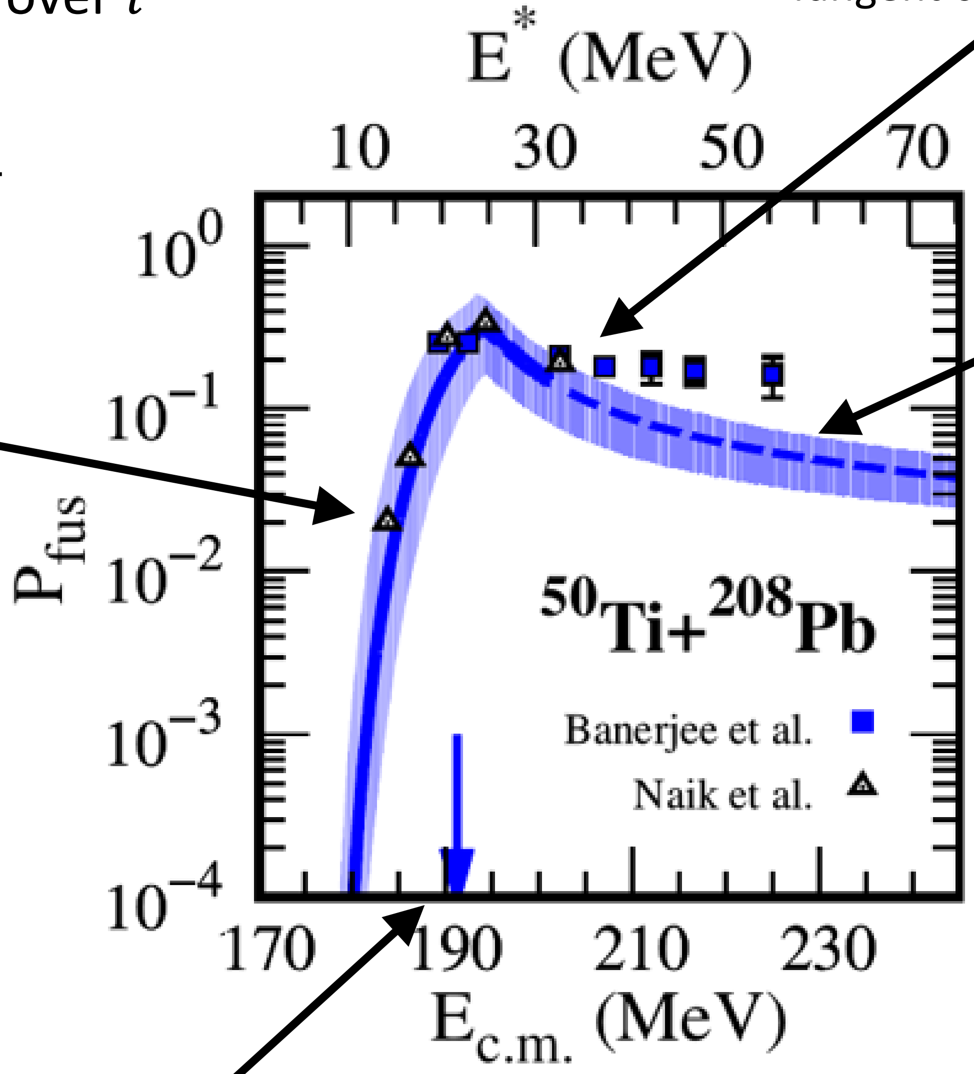

The *Pfus* saturation above *B0* results from suppression of the contributions from higher partial waves and can be linked to the critical angular momentum.

The difference between rotational energies in the fusion saddle and the contact (sticking) configuration plays a major role in CN formation at energies above *B0.*

B0 - entrance channel barrier (Coulomb+Nuclear potential)

NARODOWE CENTRUM BADAŃ JĄDROWYCH ŚWIERK

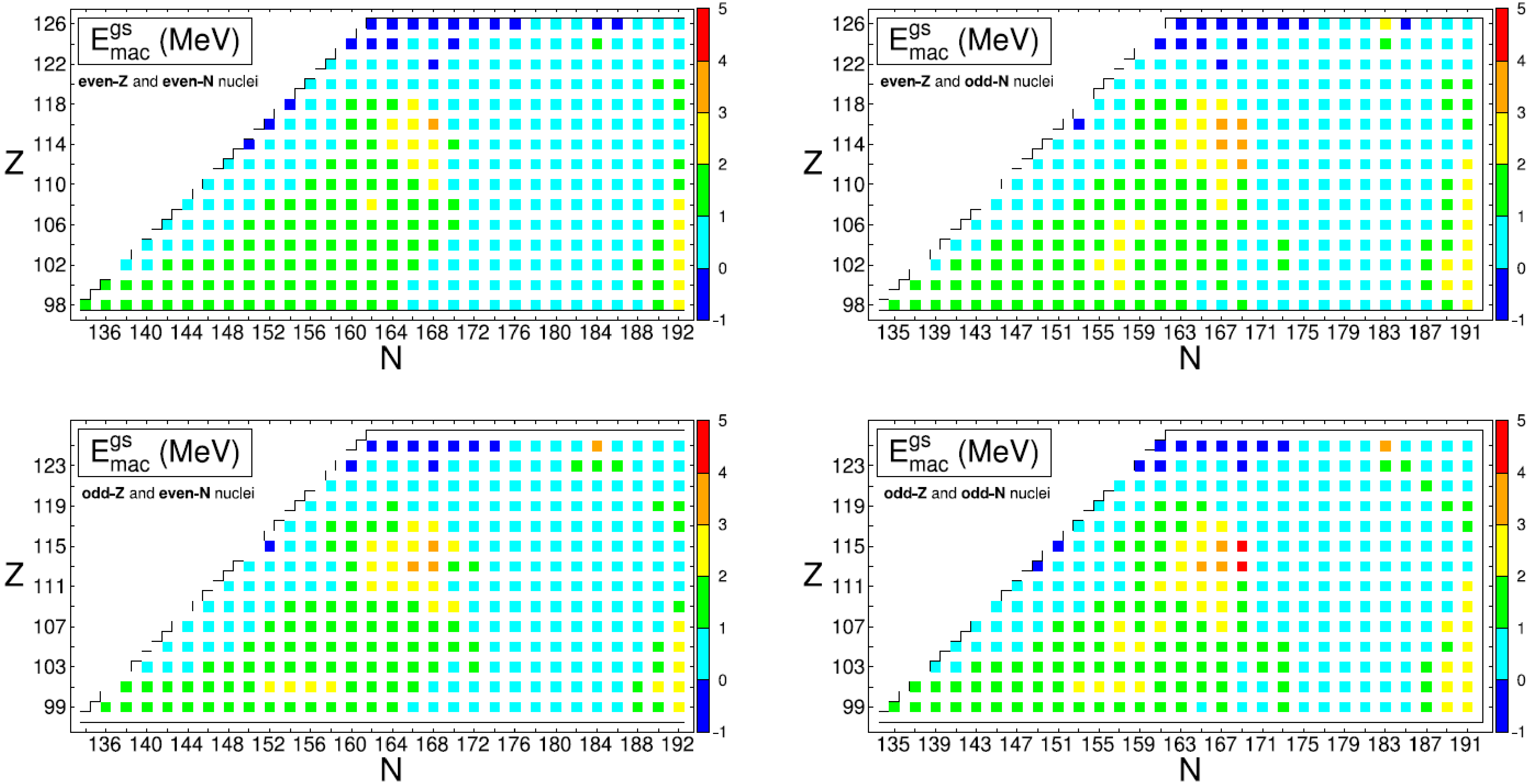

P. Jachimowicz, M. Kowal, J. Skalski, Properties of heaviest nuclei with 98≤Z≤126 and 134≤N≤192, Atomic Data and Nuclear Data Tables, Volume 138, 2021, 101393

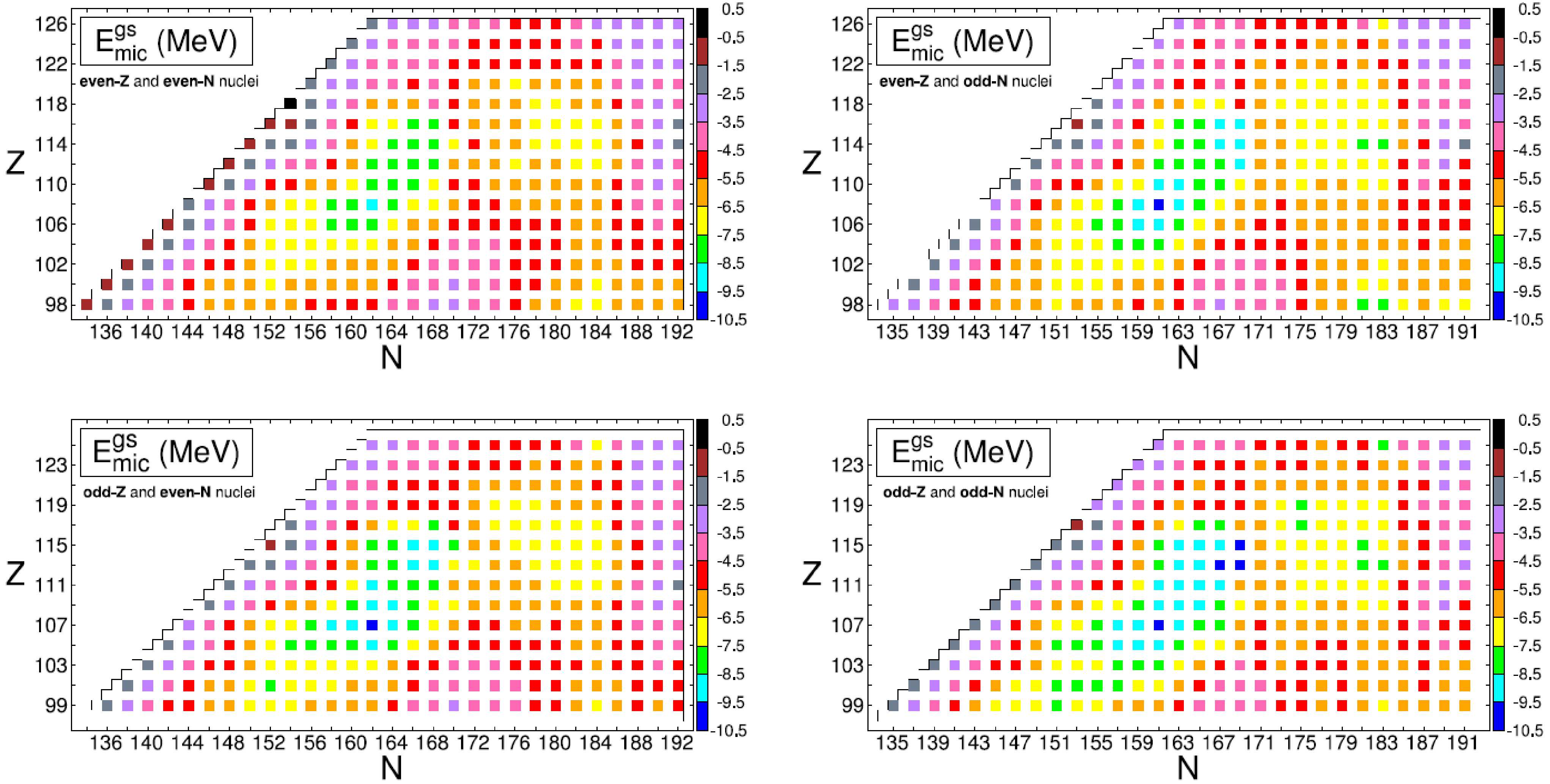

Fig. 2. Calculated microscopic component E^{gs}_{mic} of the ground state binding energy in 4 separate groups of nuclei.

P. Jachimowicz, M. Kowal, J. Skalski, Properties of heaviest nuclei with 98≤Z≤126 and 134≤N≤192, Atomic Data and Nuclear Data Tables, Volume 138, 2021, 101393

NARODOWE CENTRUM BADAŃ JĄDROWYCH ŚWIERK

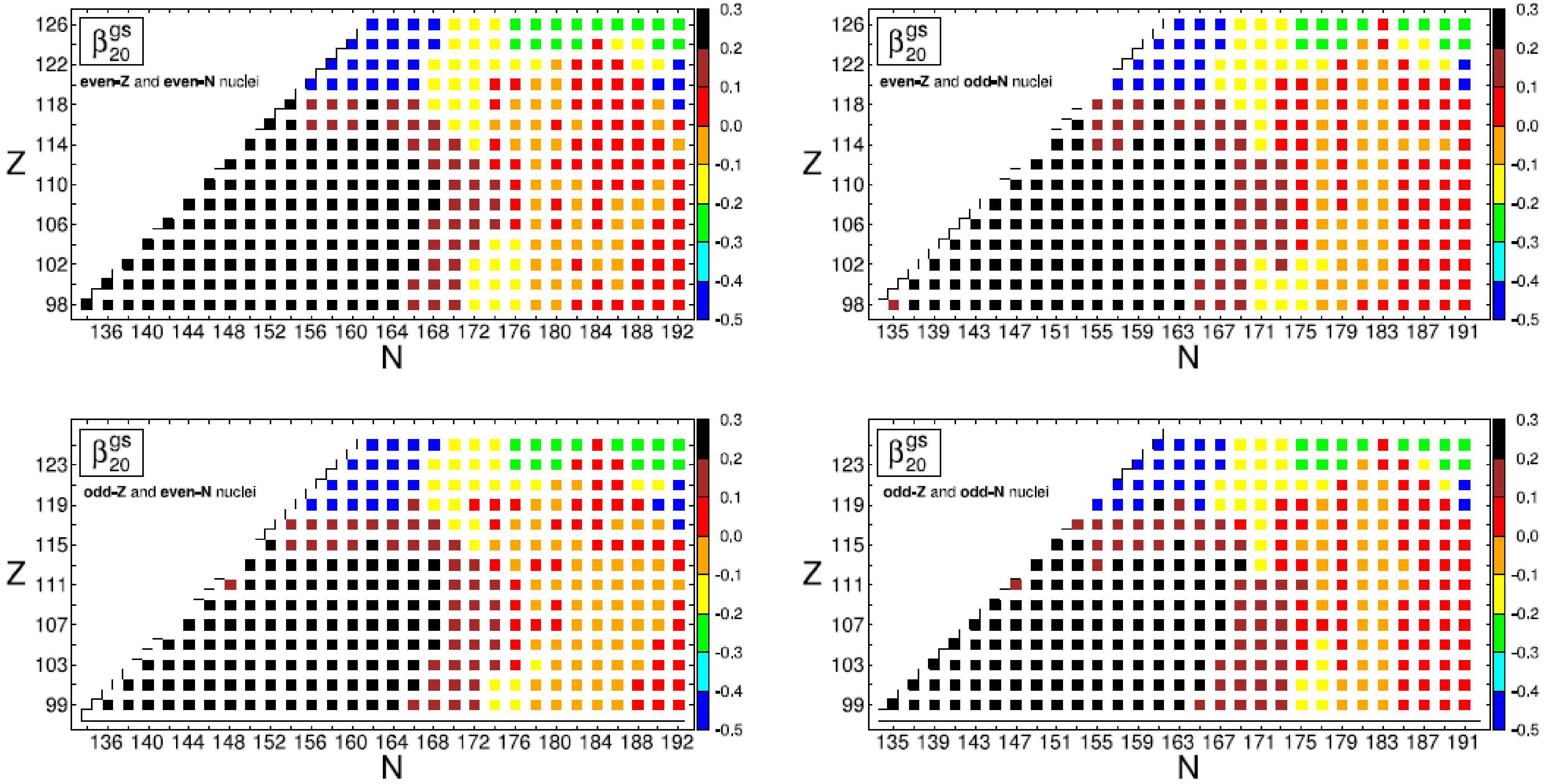

Fig. 4. Calculated ground-state quadrupole deformations β_{20}^{gs} in 4 separate groups of nuclei.

P. Jachimowicz, M. Kowal, J. Skalski, Properties of heaviest nuclei with 98≤Z≤126 and 134≤N≤192, Atomic Data and Nuclear Data Tables, Volume 138, 2021, 101393

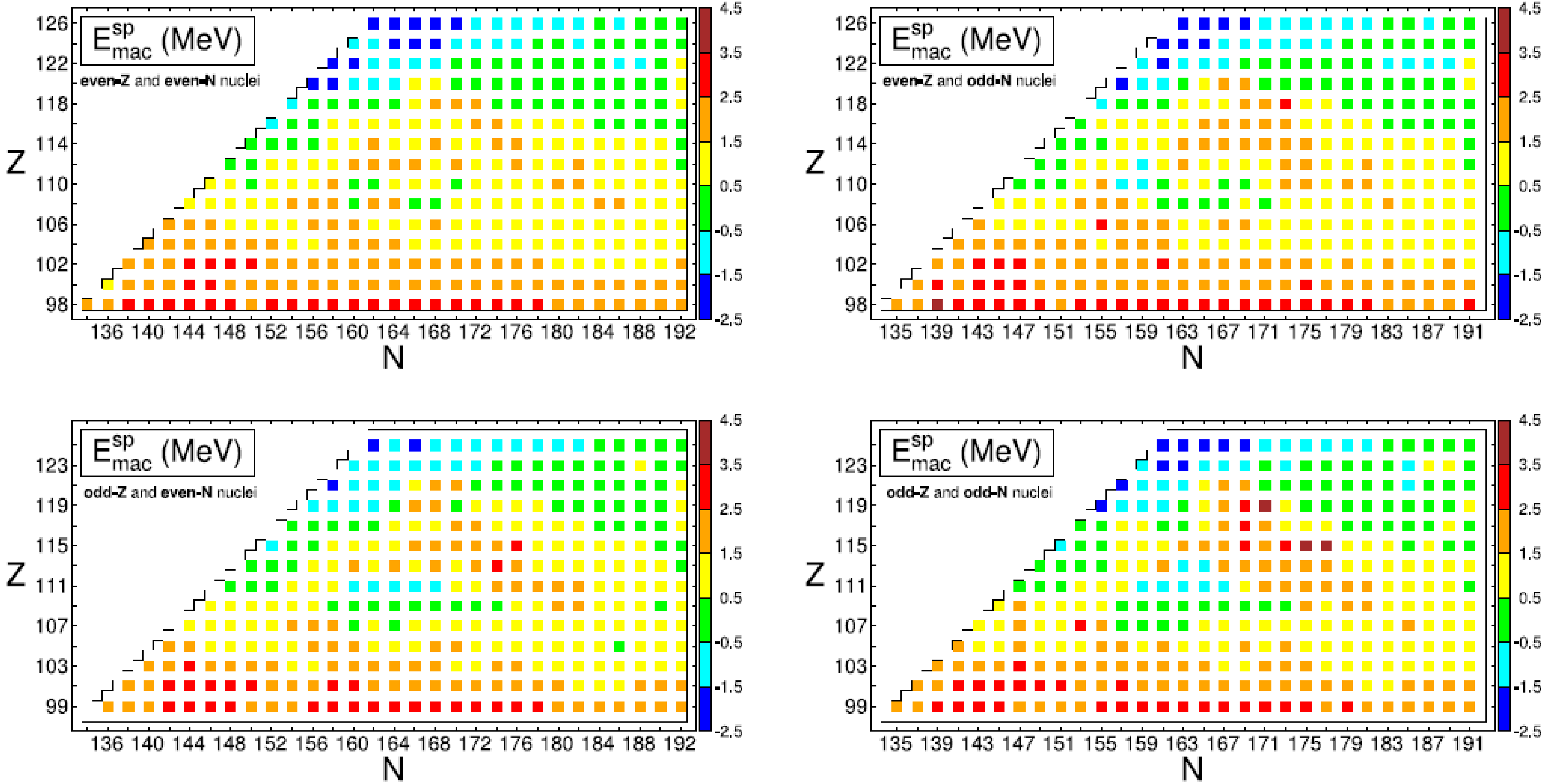

Fig. 12. As in Fig. 1, but for the calculated saddle points.

P. Jachimowicz, M. Kowal, J. Skalski, Properties of heaviest nuclei with 98≤Z≤126 and 134≤N≤192, Atomic Data and Nuclear Data Tables, Volume 138, 2021, 101393

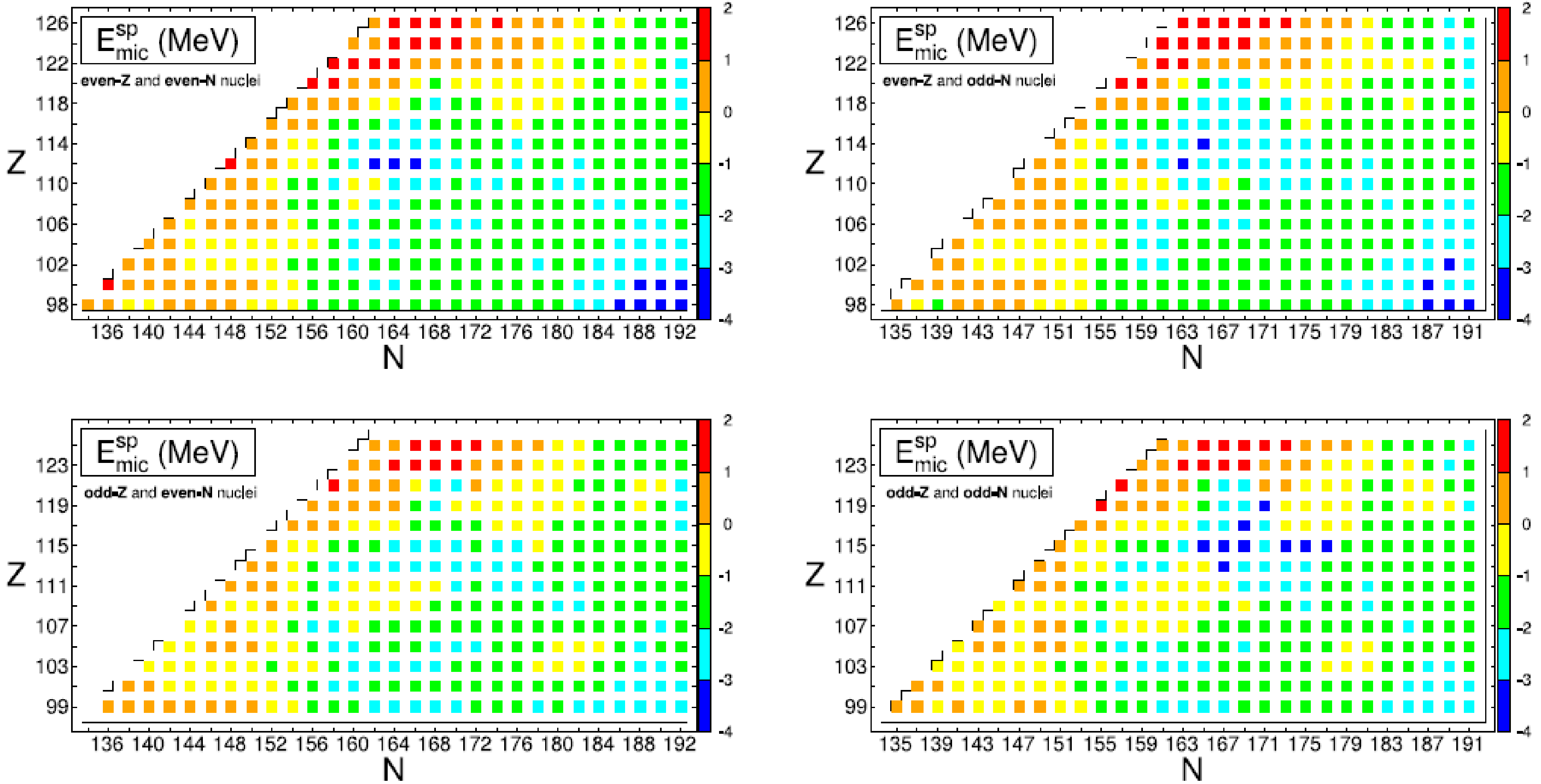

Fig. 13. As in Fig. 2, but for the calculated saddle points.

P. Jachimowicz, M. Kowal, J. Skalski, Properties of heaviest nuclei with 98≤Z≤126 and 134≤N≤192, Atomic Data and Nuclear Data Tables, Volume 138, 2021, 101393

Example of a paths

$^{54}Cr + ^{208}Pb$

$E^* = 50$ MeV, $l = 40$

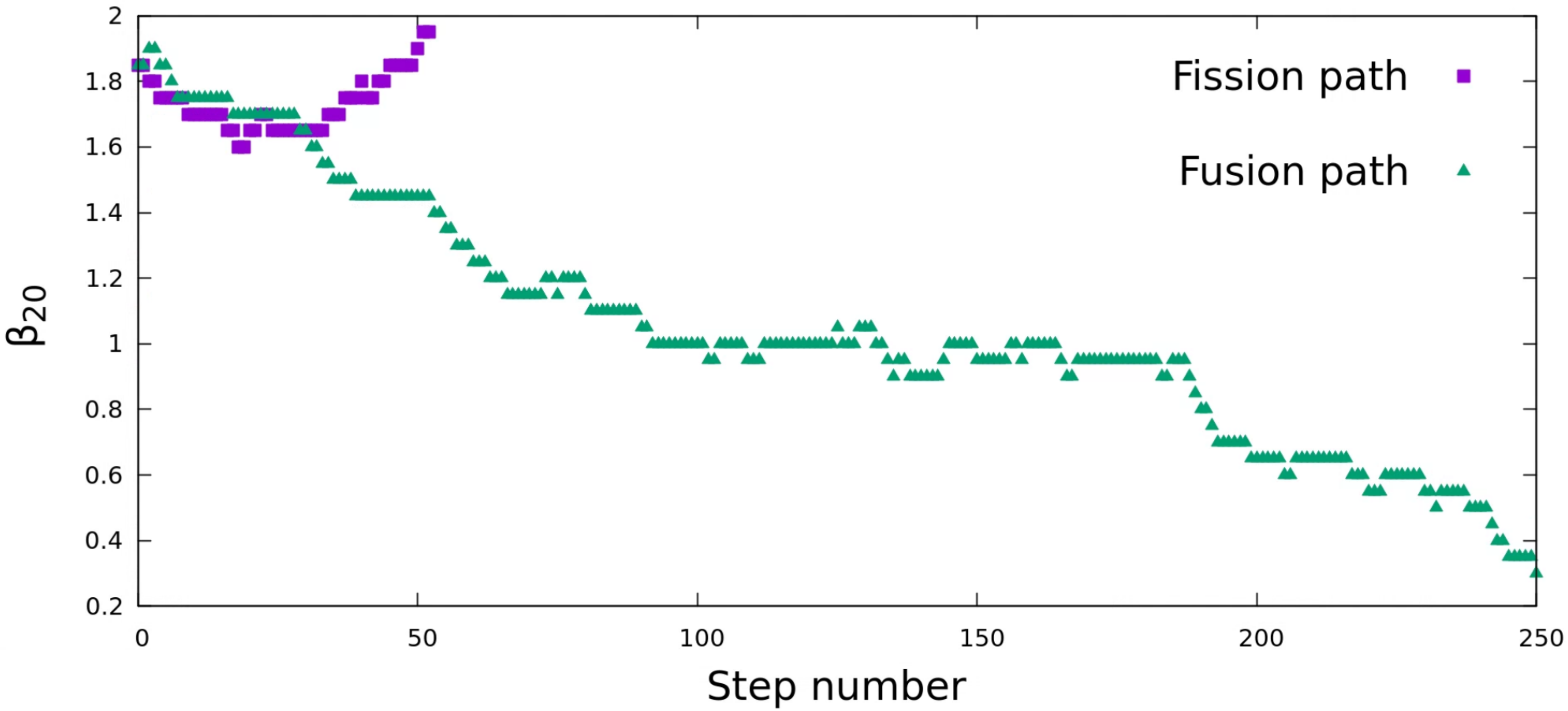

Example of a paths

$^{54}Cr + {}^{208}Pb$

$E^* = 50$ MeV, $l = 40$

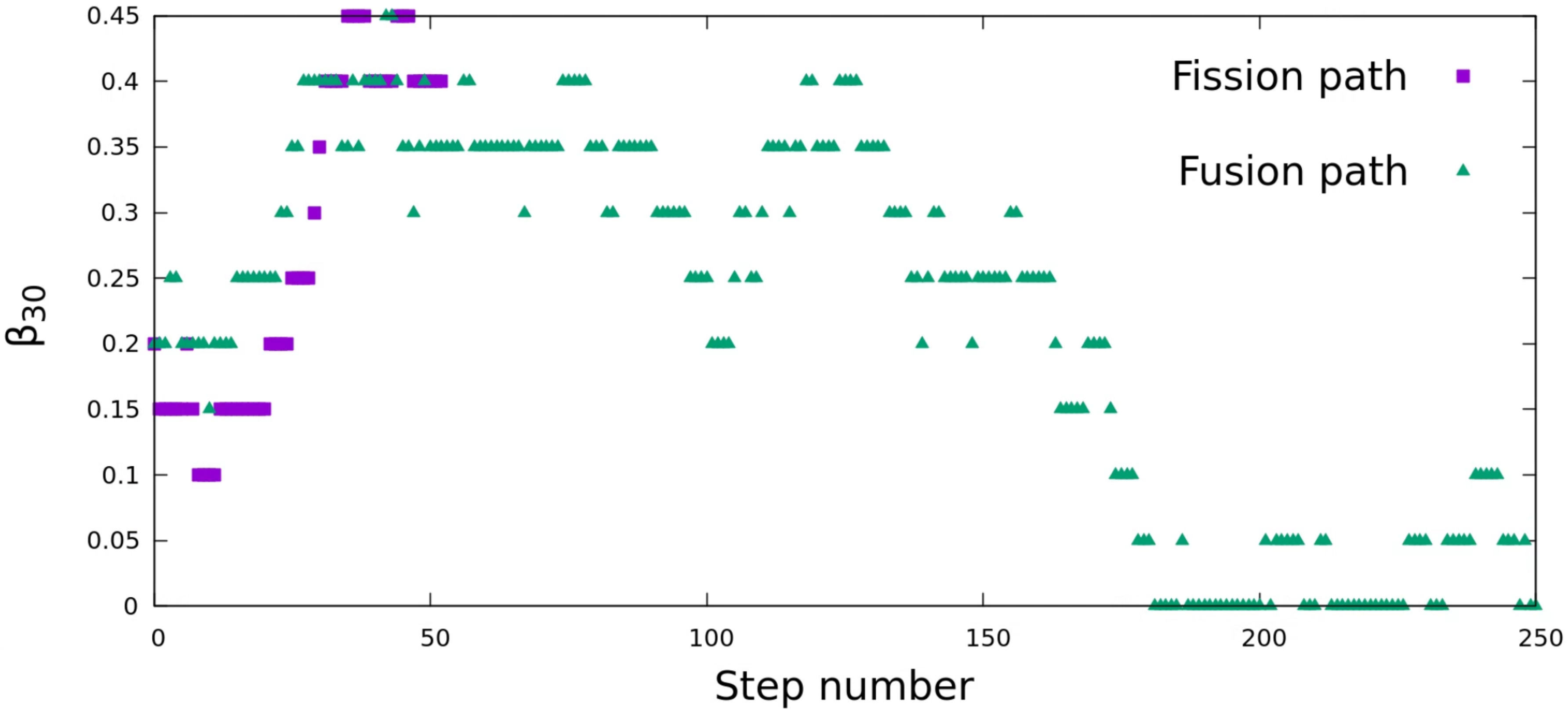

Example of a paths

$^{54}Cr + {}^{208}Pb$

$E^* = 50$ MeV, $l = 40$

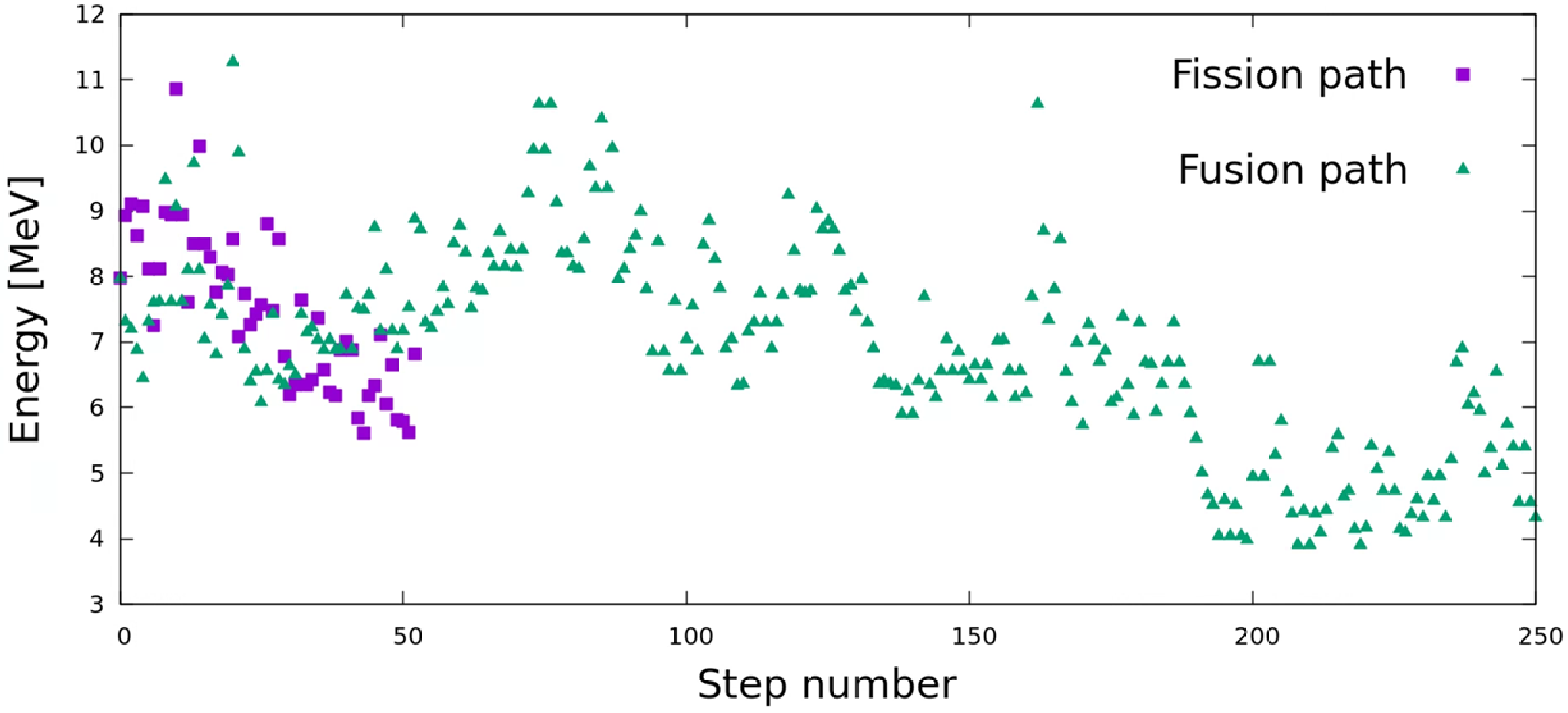

Next steps for fusion

- Expand to 8 $\beta_{\lambda 0}$ dimensions
- Determine optimal step size for each β parameter
- Expand the model to describe under barrier reactions
- Expand to non-axially symmetric shapes ($\beta_{\lambda\mu}$) and incorporate multiple possible starting points depending on the orientation of the target and the projectile
- Introduce a density parameter beyond Fermi gas model and incorporate shell-correction damping
- Allow for the emission of neutrons, protons and alfa particles during the random walk